CREEP OF GROUTED ANCHORS IN ICE-RICH SILT

BY

LIANGBIAO CHEN

RECOMMENDED:

Advisory Committee Chair

Chair, Department of Civil Engineering

APPROVED:

Dean, College of Engineering and Mines

Dean of Graduate School

May 2, 2011

Date

CREEP OF GROUTED ANCHORS IN ICE-RICH SILT

A

THESIS

Presented to the Faculty

of the University of Alaska Fairbanks

in Partial Fulfillment of the Requirements

for the Degree of

MASTER OF SCIENCE

By

Liangbiao Chen, B.S.

Fairbanks, Alaska

2011

Abstract

Creep is a critical consideration for designing anchors in ice-rich silt. In this study, creep was evaluated for grouted anchors in ice-rich silt by laboratory tests. A total of nineteen staged-load pullout tests were conducted on smooth grouted anchors. The anchors were loaded until either a tertiary creep stage or the capacity of the load system was reached. Soil temperatures evaluated in this study ranged from 32 ^{o}F to 26.6 ^{o}F. It was found that the onset of tertiary creep for smooth anchors was around 0.03 inches, which was much smaller than that suggested in the literature for rough anchors (1.0 inch). Given the same shear stress and soil temperature, the observed creep displacement rates for smooth anchors were greater than those given by the existing design guidelines for rough anchors.

A new creep model was proposed in which soil temperature was included as an additional variable. Model parameters were developed as a function of soil temperature and moisture contents by using the test data. The model predictions were compared with the laboratory tests. It was found that the creep displacement rates decreased with the decreasing of soil moisture contents and temperature. Based on the analysis of laboratory test data, design charts were provided to give the allowable pullout capacity for smooth anchors in ice-rich silt.

Table of Contents

Page

Signature Page i

Title Page ii

Abstract iii

Table of Contents iv

List of Figures vi

List of Tables ix

List of Appendices x

Acknowledgement xi

Chapter 1 Introduction 1

1.1 Objectives of the Research 1

1.2 Research Methodology 2

Chapter 2 Literature Review 3

2.1 Background on Grouted Anchors 3

2.2 Creep Behavior of Grouted Anchors 4

2.3 Factors Influencing Creep of Anchors in Permafrost 6

2.4 Existing Theories for Creep in Frozen Soil 9

2.5 Design for Anchor Capacity 14

2.6 Anchor Load Tests in Permafrost 15

Chapter 3 Anchor Load Tests and Test Results 18

3.1 Soil Preparation 18

3.2 Laboratory Creep Test Setup 19

3.3 Anchor Installation Methods 21
3.4 Testing Procedures 23
3.5 Test Results 24
Chapter 4 Data Analysis and Discussion 29
4.1 Comparison with Rough Anchors Based on the Design Guidelines 29
4.2 Development of a Time-Dependent Creep Equations 30
4.3 Effect of Soil Moisture Content and Temperature 31
4.4 Design Example 33
4.5 Design Charts 35
Chapter 5 Conclusions and Recommendations 37
5.1 Conclusions 37
5.2 Recommendations 38
References 39
Appendix A: Anchor Load Tests in the Laboratory 48
A.1 Test Anchor Configurations and Fabrications 48
A.2 Load Frame Configurations and Calibrations 51
A.3 Displacement Measurement 56
A.4 Testing Procedures 58
Appendix B: Anchor Load Test Results 63
B.1 Load Conditions 63
B.2 Creep Curves from the Nineteen Load Tests 66
Appendix C: Data Regression Results 84

List of Figures

Page

Figure 2.1 Typical configuration of a grouted anchor in permafrost. 3

Figure 2.2 Basic creep behavior of grouted anchors or piles. 5

Figure 2.3 Schematic plot of a grouted anchor subject to pullout loading. 11

Figure 2.4 Schematic displacement curve of constant-load tests. 16

Figure 2.5 Schematic displacement curve of staged-load tests 16

Figure 3.1 Materials for remolding ice-rich silt. 19

Figure 3.2 Anchor load test setup. 20

Figure 3.3 Install an anchor by layer silt placement and compaction. 21

Figure 3.4 Install an anchor in a small annular space. 22

Figure 3.5 Layout of test equipment in the cold room 23

Figure 3.6 Example of the creep curves 25

Figure 3.7 Determination of the displacement rate. 26

Figure 3.8 Pullout failure pattern. 27

Figure 4.1 Effects of soil moisture contents on anchor creep. 32

Figure 4.2 Effects of soil temperatures on anchor creep 33

Figure 4.3 Tentative design chart for ice-rich silt with M. C. = 120%. 35

Figure 4.4 Tentative design chart for ice-rich silt with M. C. = 80%. 36

Figure 4.5 Tentative design chart for ice-rich silt with M. C. = 50%. 36

Figure A. 1 Configuration of the test anchors. 49

Figure A. 2 Fabrication of the test anchors. 50

Figure A.3 Configuration of the test anchors. 51

Page

Figure A.4 Front view of the Load frame with dimensions. 52

Figure A.5 Perspective view of the load frame. 53

Figure A.6 Section of the main beam 54

Figure A.7 Section of the column. 54

Figure A.8 Section of the column of lever 54

Figure A. 9 Calibration Curves for Test Frame 1 55

Figure A. 10 Calibration Curves for Test Frame 2 56

Figure A. 11 Calibration Curves for Test Frame 3. 56

Figure A.12 The setup for creep displacement measurement. 57

Figure A.13 Calibration Curves for the LVDT 58

Figure A.14 Make an oversized hole by hot-water washing. 59

Figure A.15 Backfill the silt slurry into the annular space. 60

Figure A.16 The test anchor embedded in the unfrozen silt. 61

Figure A.17 Ice formed on the surface after the silt was frozen. 61

Figure A.18 Backfill the silt slurry into the annular space. 62

Figure B.1 Test results for test #1-120. 66

Figure B.2 Test results for test #2-120. 67

Figure B.3 Test results for test #2-80. 68

Figure B.4 Test results for test #2-50. 69

Figure B.5 Test results for test #3-120. 70

Figure B.6 Test results for test #3-80. 71

Figure B.7 Test results for test #3-80. 72

Page

Figure B.8 Test results for test #4-120. 73

Figure B.9 Test results for test #4-80. 74

Figure B.10 Test results for test #4-50. 75

Figure B.11Test results for test #5-120. 76

Figure B.12 Test results for test #5-80. 77

Figure B.13 Test results for test #5-50. 78

Figure B.14Test results for Test # 6-120. 79

Figure B.15 Test results for Test # 6-80. 79

Figure B.16 Test results for Test # 6-50. 80

Figure B.17 Test results for test #7-120. 81

Figure B.18 Test results for test #7-80. 82

Figure B.19 Test results for test #7-50. 83

Figure C.1 Regression result for M.C. = 120%. 84

Figure C.2 Regression result for M.C. = 80%. 84

Figure C.3 Regression result for M.C. 50%. 85

List of Tables

Page

Table 2.1 Summary of influencing factor on anchor or pile creep. 9

Table 2.2 Creep parameters in the design guidelines. 14

Table 2.3 Creep parameters based on the load tests in the literature. 17

Table 3.1 Summary of displacement rates. 28

Table 4.1 Test results versus prediction by the existing design guidelines. 29

Table 4.2 Summary of the regression analysis. 31

Table A. 1 Summary of the load frame elements. 55

Table B.1 Loading conditions for nineteen anchor load tests. 64

List of Appendices

Page

Appendix A: Anchor Load Tests in the Laboratory 48

A.1 Test Anchor Configurations and Fabrications 48

A.2 Load Frame Configurations and Calibrations 51

A.3 Displacement Measurement 56

A.4 Testing Procedures 58

Appendix B: Anchor Load Test Results 63

B.1 Load Conditions 63

B.1 Creep Curves from the Nineteen Load Tests 66

Appendix C: Data Regression Results 84

Acknowledgement

I wish to thank my advisors, Dr. Xiong Zhang and Mr. Billy Connor, for being my committee chairman and spending considerable time guiding me on the research. I would also like to thank Drs. Yuri Shur and Dr. Leroy Hulsey, for serving as my committee members and for their continuous professional support on experimental research of anchors in permafrost. I would like to thank the lab manager, Gary Tyndall for the help with my laboratory work.

I want to give special thanks to Alaska Department of Transportation & Public Facilities and Alaska University Transportation Center, who made this work possible through their funding support. Their support is especially appreciated.

I also want to thank all of my friends in the Department of Civil and Environmental Engineering at the University of Alaska Fairbanks.

Chapter 1 Introduction

Grouted anchors and anchored systems offer many advantages over conventional systems and have been used in unfrozen soils successfully for highway application for decades. They may be an alternative means to mitigate the problems associated with ice-rich permafrost that was exposed and thawed during road construction operation. It is well known that ice-rich soils have creep behavior under constant loading. This is also one of the major concerns for practitioners when design anchors in ice-rich soils. In order to investigate the applicability of anchored systems in Alaska's harsh climate, creep of grouted anchors in ice-rich permafrost needs to be evaluated. Prior to this research, the existing design guidelines do not provide the engineer with a relationship between minimum displacement rates and applied shear stresses as a function of soil temperatures and soil moisture contents for grouted anchors in ice-rich silt.

1.1 Objectives of the Research

The primary focus of this study was to evaluate the creep of straight-shafted grouted anchors in ice-rich silt. The major objectives of this research were listed as follows:

1. Exploration of the existing creep theory and design guidelines for grouted anchors in permafrost;
2. Development of an experimental method to monitor creep displacement of grouted anchors in ice-rich silt at different temperatures;
3. Development of the relation between minimum displacement rates and applied shear stresses at different soil temperatures.

4. Investigation of the effects of soil temperatures and moisture contents on creep of grouted anchors in ice-rich silt;
5. Development of design charts for grouted anchors in ice-rich silt.

1.2 Research Methodology

To achieve the objectives of this study, the following tasks were conducted:

1. Literature review. —Chapter 2 provided background information on grouted anchors in permafrost. It also presented the creep theory, design guidelines and basic load tests for grouted anchors.
2. Anchor load tests. —Chapter 3 described the test equipment and procedures used to conduct laboratory based anchor load tests. A summary of these test results was also presented.
3. Data analysis. —In Chapter 4, test results were first compared with the existing design guidelines. Regression analysis was then conducted to establish the minimum displacement rate relationship for smooth anchors in ice-rich silt. Based on the regression equations, the effects of soil temperatures and moisture content on anchor creep were discussed. Design examples and design charts were also given.
4. Conclusions and recommendations. —Upon completing the anchor load tests and the data analysis, results were synthesized to draw conclusions and recommendations. These were presented in Chapter 5.

Chapter 2 Literature Review

2.1 Background on Grouted Anchors

The use of grouted anchors in permafrost dates back to the 1970s (Johnston and Ladanyi, 1972). Grouted anchors were primarily used as anchorages for guyed towers, or buried pipelines in cold regions. In unfrozen soil, grouted anchors were usually used for retaining walls. They are used widely for various engineer structures and have been proved more cost-effective than other retaining systems (Power and Briaud, 1993).

As shown in Figure 2.1, a grouted anchor is essentially a steel tendon (e.g., threaded

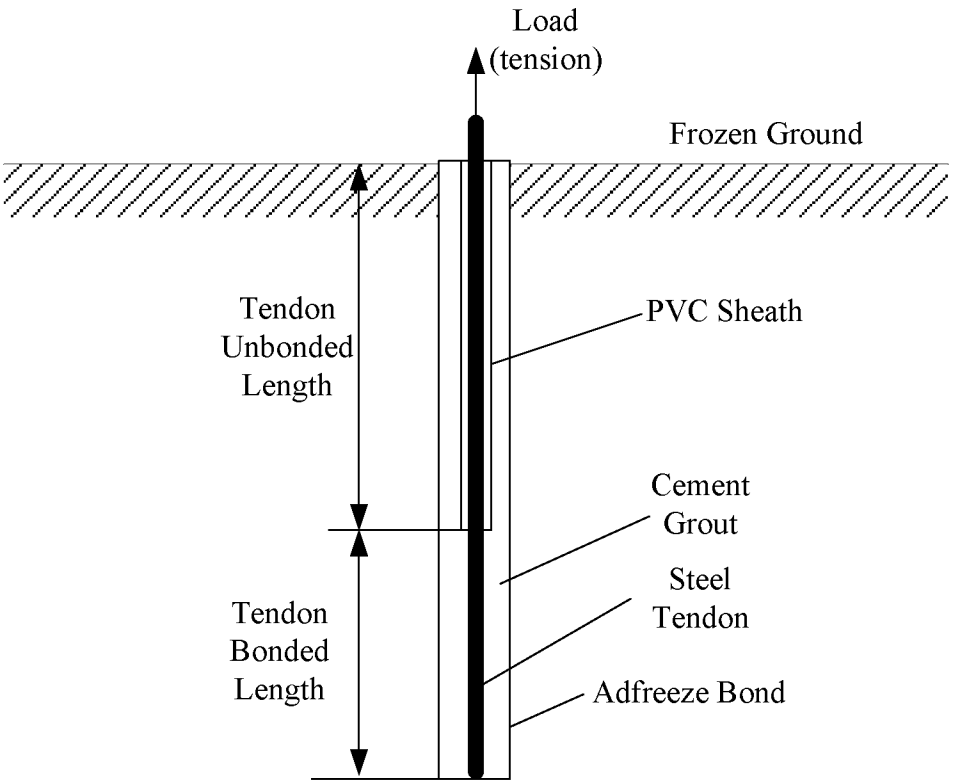

Figure 2.1 Typical configuration of a grouted anchor in permafrost.

bar) secured in the ground by cement grout (Power and Briaud, 1993). It is installed first by placing steel tendon into a pilot hole and then by filling the hole with grout materials. In frozen ground, rapid setting cement was suggested for use to mitigate degradation of frozen soils (Biggar and Sego 1990). Usually, a tensile load is applied to anchor head and then transferred from the steel tendon to the grout through the tendon-bonded length (Figure 2.1). For tendon-unbonded length, a greased PVC sheath is usually installed to prevent the bonding between cement grout and steel tendon. The applied load on the anchor head is transferred to the ground by adfreeze bond along the grout shaft. This behavior is similar to frictional piles subjected to tensile loads, as indicated in the literature (e.g., Jonston and Ladanyi, 1972; Andersland and Ladanyi, 2004).

2.2 Creep Behavior of Grouted Anchors

In cold regions, grouted anchors under constant loads are usually subjected to time dependent displacement, or creep. Creep of anchors or piles has been observed in both the field and in laboratory tests and may be a critical consideration for the practical design (Johnston and Ladanyi, 1972; Biggar and Kong, 2001).

Figure 2.2a illustrates schematically a typical creep curve (displacement versus time) of grouted anchors under constant load. Figure 2.2b shows the displacement rate versus time curve for the creep curve in Figure 2.2a. In general, three distinguished stages may occur in a creep curve: primary, secondary, and tertiary creep. Primary

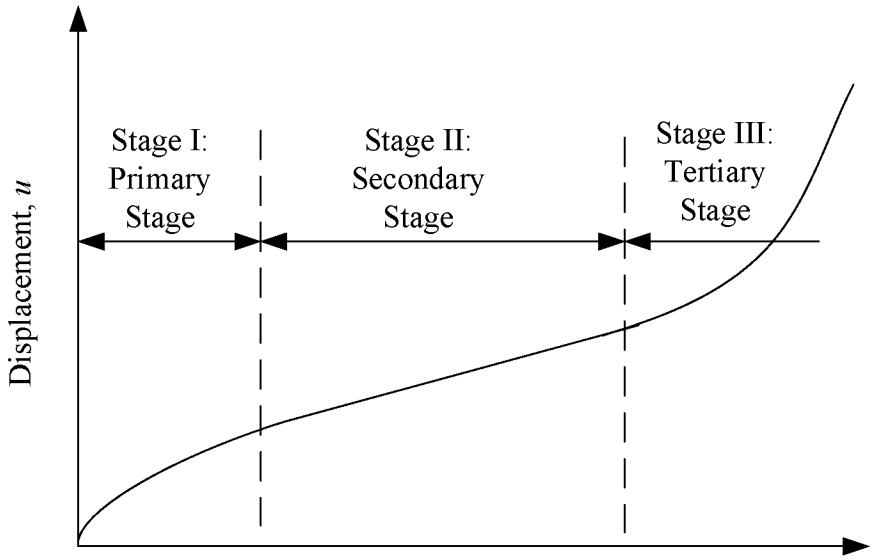

(a)

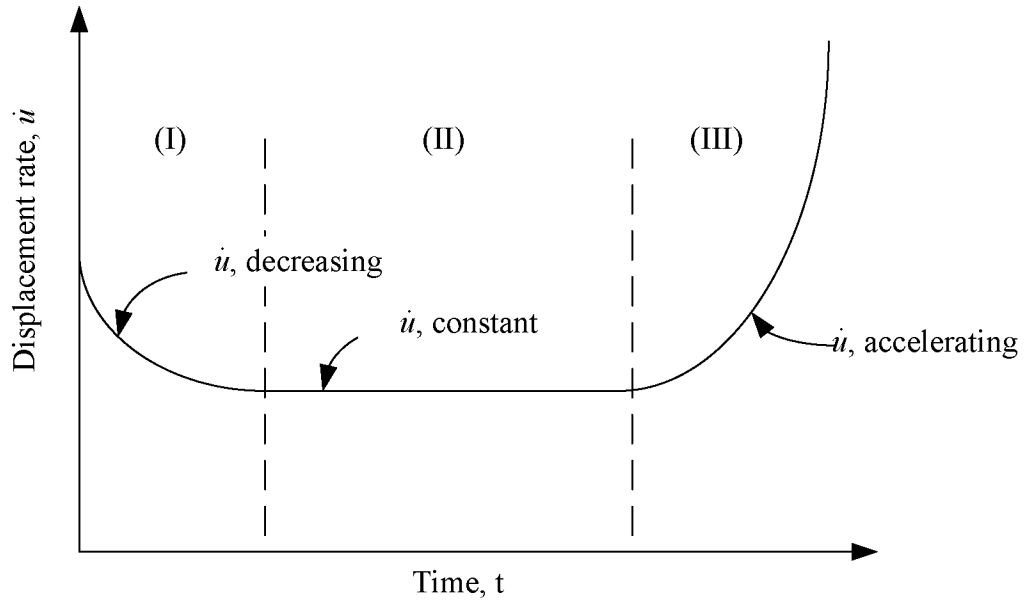

(b)

Figure 2.2 Basic creep behavior of grouted anchors or piles. (After Vialov, 1959; Biggar and Kong, 2001)

creep is characterized by decreasing displacement rate, secondary by constant displacement rate, and tertiary by accelerating displacement rate. Occurrence of creep stages and magnitudes of creep displacement rate are dependent on the factors such as load levels, soil types and temperatures. These factors are to be discussed in Section 2.3.

2.3 Factors Influencing Creep of Anchors in Permafrost

At present studies on the creep of grouted anchors in permafrost are still scarce. In addition, majority of available literatures (e.g., Johnston and Ladanyi, 1972; Biggar, 1991) mainly focus on ice-poor soil (the soil with water content below 50% by weight). By contrast, literatures on creep for piles are numerous for both ice-poor and ice-rich soil (the soil with water content above 50%). As discussed previously, piles and grouted anchors share similar creep mechanism. Consequently, the findings for piles can provide useful information for the research on grouted anchors. From the existing literatures on pile foundations in permafrost, it was found that factors that influence the creep behavior for anchors or piles in frozen soils generally included:

1. Applied shear stress. —Increasing applied shear stress along the anchor shaft may cause greater creep displacement or displacement rate (Vialov, 1959). At low stress (e.g., 20% of ultimate shear strength), anchor displacement may undergo just primary creep or secondary creep. At high shear stresses (e.g., 80% of ultimate shear strength), anchor displacement may go quickly into the tertiary

creep stage followed by the failure of the anchor.

2. Soil temperature. —Soil temperature has been shown to have great impact on creep behavior of anchors. Generally, the creep displacement rate decreases as soil temperature drops. For example, Morgenstern, et al. (1980) found that given the same shear stress and pile diameter, displacement rates at 14 ^{o}F (-10.0 ^{o}C) may be 10 to 100 times less than those at 30.2 ^{o}F (-1.0 ^{o}C). Similar results were also found by Nixon and Neukirchner (1984), who studied the creep of piles in ice-rich, saline permafrost for temperature between 23 ^{o}F and 14 ^{o}F.
3. Salinity of soils. —The effects of salinity on the creep of grouted piles have been widely investigated (e.g., Nixon and Neukirchner, 1984; Biggar and Sego, 1993b, 1994; Biggar and Kong, 2001). According to the literature, displacement rates of grouted piles in a high-salinity soil can be thousands of times greater than those in a low-salinity soil.
4. Pile surface roughness. —Corrugated anchors may reach the tertiary creep at a displacement limit up to 25 mm (Johnston and Ladanyi, 1972). For smooth anchors or piles, however, the displacement limit may be just several millimeters (Andersland and Ladanyi, 2004). The displacement limit may increase up to 15mm by installing lugs on smooth steel piles (Stelzer and Andersland, 1989).
5. Backfill material. — Backfill material is used when an anchor or pile is installed in an over-sized hole. The actual surface area of the pile may increase if the failure surface occurs at the interface of the backfilled material and native soils.

Different backfill materials may have various effects on the creep of anchors or piles. Compared with backfills made of sand, backfills made of cement grout may reduce the displacement rate of piles (Biggar, 1991).

6. Pile installation methods. —Vialov (1959) examined the performance of wood piles in frozen soils and found that frozen-in wood rods showed greater creep than driven-in ones. The frozen-in rods were installed in oversized holes and backfilled with soil slurry. While the driven-in piles were installed by driving the pile into a small pilot hole.
7. Ice content. —Generally, piles in ice-rich soil demonstrate greater creep those in ice-poor soil. Biggar (1991) reported that piles in ice-poor soils exhibited mainly primary creep while piles in ice-rich soils demonstrated mainly secondary creep.

Table 2.1 summarizes the influencing factors discussed above. Generally, creep of anchors in frozen soil may be affected by properties of surrounding soils, soil temperature and conditions of the anchor-soil interface.

Table 2.1 Summary of influencing factor on anchor or pile creep.

Influencing Factor	Conditions	Creep Rate	Sources
applied stress	80% of ultimate strength	high	Vialov, 1959
	20% of ultimate strength	low	
temperature	warm	high	Morgenstern et al., 1980
	cold	low	
salinity of soils	high	high	Biggar and Sego, 1993b
	low	low	
surface roughness	smooth	high	Stelzer and Andersland (1989)
	rough	low	
backfilled material	sand	high	Biggar and Sego, 1994
	grout	low	
installation method	frozen in	high	Vialov, 1959
	driven in	low	
ice content	ice-poor	primary	Biggar, 1991
	ice-rich	secondary	

2.4 Existing Theories for Creep in Frozen Soil

Some researchers investigated the creep behavior of grouted anchors or piles, such as Vialov (1959), Johnston and Ladanyi (1972, Ladanyi and Johnston (1974), Nixon and McRoberts (1976), Weaver and Morgenstern (1981), and Biggar (1991). Some common assumptions used in the studies of creep behavior of grouted anchors are as follows:

1. Weight of the anchor and soil is neglected;
2. The shear stress is uniformly distributed along the anchor;
3. The soil temperature is constant;
4. The anchor is much more rigid than the surrounding soil;
5. There is no slip between anchor and frozen soil, and

6. The frozen soil is considered incompressible.

Figure 2.3 shows an anchor subjected to a constant tensile load in frozen soil, where P represents constant tensile load, τ represents the shear stresses of frozen soil, r the distance from the anchor axis, L anchor embedment, and a anchor radius. Vertical displacement and shear distortion of frozen soil are denoted by u and γ, respectively. Displacement of the anchor is denoted by u_a.

By considering the force equilibrium in the vertical direction as shown in Figure 2.3, the shear stress, τ, of a soil element at a distance of r from the center of the grouted anchor, can be expressed as follows (Ladanyi and Johnston, 1972):

$$\tau = \tau_a \frac{a}{r} \tag{2.1}$$

where τ_a is the shear stress on the soil-anchor interface(at $r = a$). According to assumption 2, the shear stress is uniformly distributed along the anchor. Consequently, τ_a can also be calculated as follows (Nixon and McRoberts, 1976):

$$\tau_a = \frac{P}{2\pi aL} \tag{2.2}$$

For frozen soil subjected to the creep behavior due to the simple shear, the relationship between the shear strain, γ, shear stress, τ, and time, t, can be expressed by the following equation (Ladanyi, 1972; Biggar, 1991):

$$\gamma = \sqrt{3^{(c+1)}} D\tau^c t^b \tag{2.3}$$

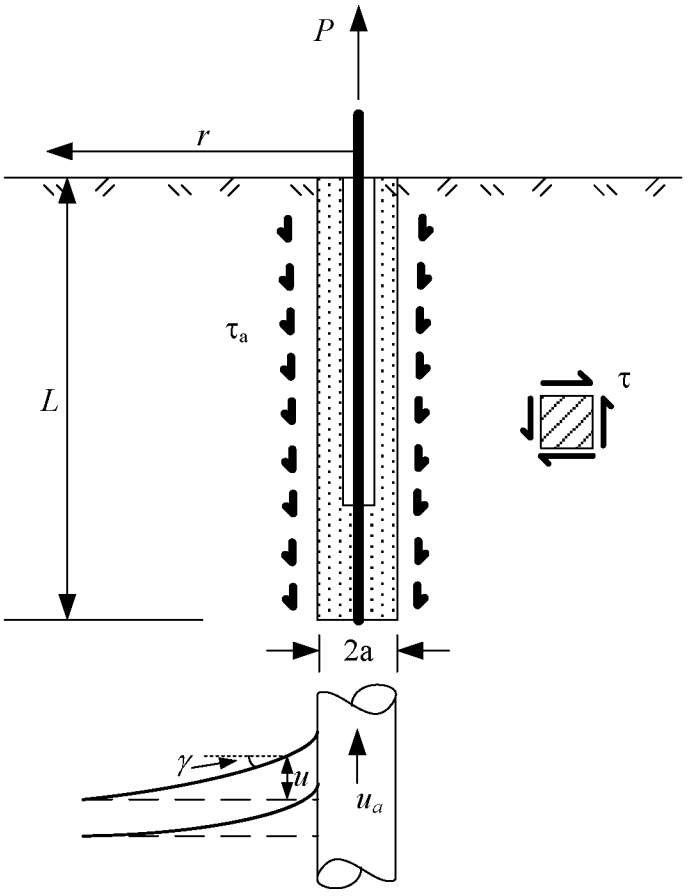

Figure 2.3 Schematic plot of a grouted anchor subject to pullout loading. (Modified from Johnston and Ladanyi, 1972; Nixon and McRoberts, 1976)

where c is the creep exponent for stress, b is the time exponent, and D is the parameter dependent on material properties and temperature. Substituting Equation 2.1 into the Equation 2.3 yields (Biggar, 1991):

$$\gamma = \sqrt{3^{(c+1)}} D \cdot \left(\tau_a \frac{a}{r} \right)^c t^b \tag{2.4}$$

On the other hand, the shear strain of the soil element can be expressed as follows (Nixon and McRoberts, 1976):

$$\gamma = -\frac{du}{dr} \tag{2.5}$$

By combining Equations 2.4 and 2.5, one has (Biggar, 1991):

$$\frac{du}{dr} = -\sqrt{3^{(c+1)}} D \cdot \left(\tau_a \frac{a}{r} \right)^c t^b \tag{2.6}$$

The boundary conditions are: at $r = \infty, u = u_a$ and at $r = \infty, u = 0$. Solving Equation 2.6 yields using the above two boundary conditions, the following equation is obtained (Nixon and McRoberts, 1976; Biggar, 1991):

$$u_a = \frac{\sqrt{3^{(c+1)}} D \cdot \tau_a^c \cdot a \cdot t^b}{(c-1)} \tag{2.7}$$

Equation 2.7 is usually expressed as follows (Nixon and McRoberts, 1976):

$$\frac{u_a}{a} = \frac{\sqrt{3^{(c+1)}} D \cdot \tau_a^c \cdot t^b}{(c-1)} \tag{2.8}$$

where $\frac{u_a}{a}$ is defined as the normalized displacement. When b<1, and c>1, Equation 2.8 represents the primary creep with an attenuating displacement rate, which is usually observed for piles in ice-poor soils. When b=1, and c>1, Equation 2.8 represents the secondary creep with constant displacement rate, which is usually

observed for piles in ice-rich soils (Biggar, 1991).

By assuming b=1, Morgenstern et al., (1980) and Weaver (1979) proposed a formulation similar to Equation 2.8 as follows:

$$\frac{u_a}{a} = \frac{\sqrt{3^{(n+1)}} B \cdot \tau_a^n \cdot t}{n-1} \tag{2.9}$$

where n and B are creep parameters of frozen soils or ice, which are c and D in Equation 2.8 respectively. By taking the first derivative of u_a with respect to time t, Equation 2.9 becomes (Biggar, 1991):

$$\frac{\dot{u}_a}{a} = \frac{\sqrt{3^{(n+1)}} B \cdot \tau_a^n}{n-1} \tag{2.10}$$

where the unit for the left term (normalized displacement rate) is the inverse of time (e.g., inch/year/inch= year^{-1}). Morgenstern et al.(1980) proposed that Equation 2.10 be used to predicate displacement rate of rough piles in ice-rich soil. They also suggested values of n and B for different temperatures as shown in Table 2.2. However, some researchers reported that using creep parameters in Table 2.2 may result in conservative designs for piles in ice-rich soil (Weaver and Morgenstern, 1981; Phukan, 1985).

Table 2.2 Creep parameters in the design guidelines. (Morgenstern et al., 1980).

Temperature, °F	n	B (kPa^{-n} year^{-1})
30.2	3.0	4.50×10^{-08}
28.4	3.0	2.00×10^{-08}
23	3.0	1.00×10^{-08}
14	3.0	5.60×10^{-09}

2.5 Design for Anchor Capacity

As discussed previously, the working mechanisms of a grouted anchor are similar to those of axially loaded piles. As a result, it is suggested in this research that design of grouted anchors in frozen soil should follow the methods for axially loaded piles in the same soil, as suggested by Andersland and Ladanyi (2004). A basic equation for computing allowable pullout capacity for anchor or pile in frozen soil is:

$$P_{all} = 2\pi aL\tau_{a,all} + W_a \tag{2.11}$$

where P_{all} is the allowable pullout capacity for anchor, a anchor radius, L effective anchor embedment, $\tau_{a,all}$ allowable adfreeze stress (shear stress), W_a the anchor weight. The weight of anchor is usually neglected.

There are two methods for determination of $\tau_{a,all}$. One method is to first select ultimate adfreeze stress based on the published ultimate adfreeze strength and then an appropriate safety factor, usually 2.0 or 3.0, is applied to calculate the $\tau_{a,all}$ (Andersland and Ladanyi, 2004). Safety factors are used to ensure an allowable displacement. In this case, the displacement rate should be evaluated by Equation 2.10.

The other method is to select an allowable displacement rate, $\dot{u}_{a,all}$, and use the following equation to determine the allowable shear stress:

$$\tau_{a,all} = \frac{(n-1)^{1/n}}{\sqrt{3^{(n+1)/n}}B^{1/n}}\left(\frac{\dot{u}_{a,all}}{a}\right)^{1/n} \tag{2.12}$$

Equation 2.12 is obtained by rearranging Equation 2.10 to express shear stress as a function of displacement rate. The values of allowable displacement rates are dependent on various design conditions. According to Biggar (1991), normal allowable displacement rate is from 0.1 per year to approximately 0.01 per year. It was suggested parameters, n and B, can be obtained from Table 2.2, which may offer some safety margin by using ice creep data for ice-rich soil.

2.6 Anchor Load Tests in Permafrost

Equations 2.10 can be validated by two basic load tests: constant-load pullout tests and staged-load pullout tests. Typical load-displacement curves for each type of load tests are schematically shown in Figure 2.4 and 2.5, respectively. In constant-load pullout tests, a series of anchors are subjected to different constant loads and may undergo different creep stages. Those anchors which reach a secondary creep stage are analyzed to determine the creep parameters (e.g., n and B) in Equation 2.10. In the second type of load tests, known as staged-load pullout tests, only one anchor is tested but subjected to successive loads which increase in stages of different or equal duration. Those load stages in which the anchor reaches secondary creep will be

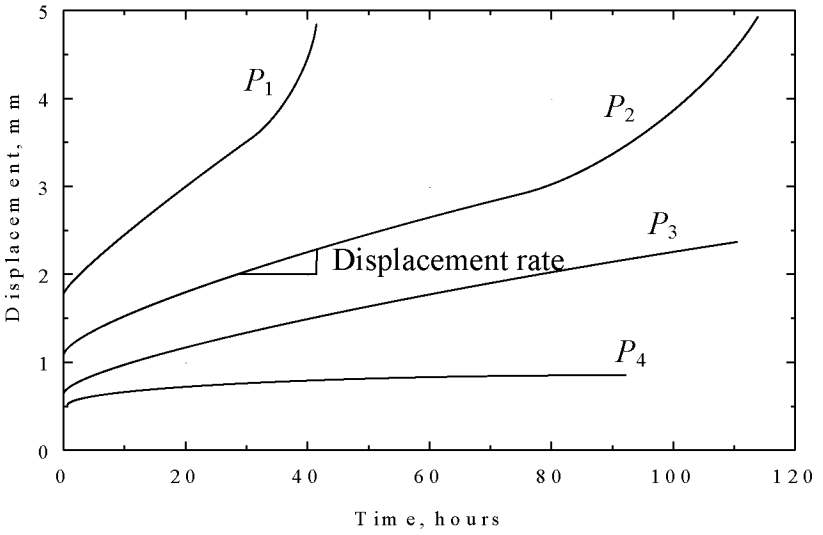

Figure 2.4 Schematic displacement curve of constant-load tests. (P_1>P_2>P_3>P_4).

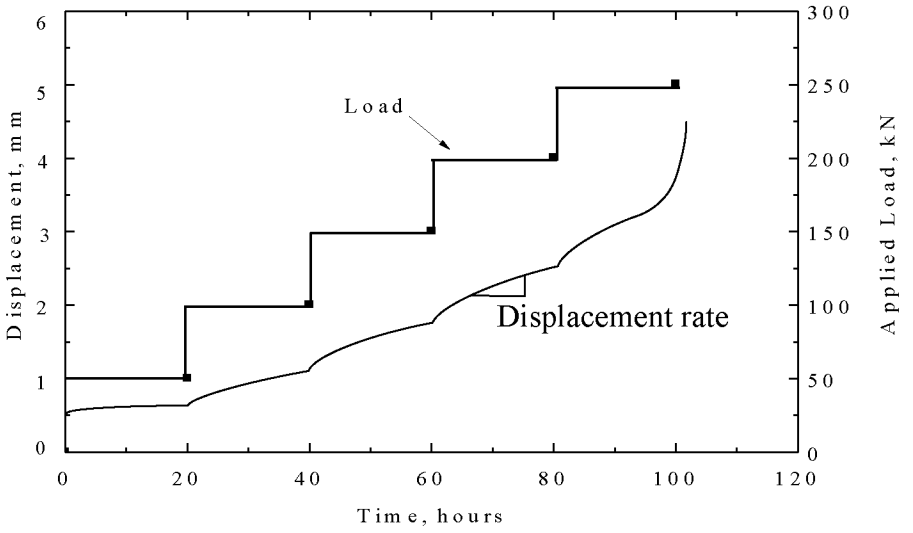

Figure 2.5 Schematic displacement curve of staged-load tests.

analyzed. According to Andersland and Johnston (2004), staged-load pullout tests are more economical than constant-load pullout tests.

Table 2.3 summarizes the creep parameters based on the studies by Johnston and Ladanyi (1972), and Biggar and Sego (1994). Compared with Table 2.2, Table 2.3 shows greater stress exponents, n, and smaller creep parameter, B. In addition, the projects presented in Table 2.3 produced different creep parameters because of different soil types and temperatures. Thus, Creep parameters should be determined by performing anchor load tests in the field if anchor creep is a major concern.

Table 2.3 Creep parameters based on the load tests in the literature.

Anchor Types	Soil Description	Temp. ^{o}F	n	B kPa^{-n} /year	Sources
Grouted Anchors	Clay and Silt M.C. 20%~50%	31	8.1	3.96×10^{-13}	Field Tests by Johnston and Ladanyi,1972
	Clay and Silt M.C. 20%~60%	31.5	7.5	5.18×10^{-12}	
Grouted Piles	Saline (30 ppt), Ice poor soils	23	9.3	1.69×10^{-25}	Laboratory tests by Biggar and Sego, 1994

Chapter 3 Anchor Load Tests and Test Results

In Chapter 2, a literature review on creep of grouted anchors in permafrost was presented. In this Chapter, the laboratory load test procedures were presented and the test results were summarized. Section 3.1 described the processes used to prepare ice-rich silt for a laboratory test. The test equipment was described in Section 3.2. Section 3.3 described the method used to install the anchor for a laboratory test. Section 3.4 provided general descriptions on testing arrangement and procedures. Test results were summarized in Section 3.5.

3.1 Soil Preparation

In this study, test anchors were installed in remolded ice-rich silt that was fabricated in the laboratory. Slurry was made by mixing dry silt, water and 20% to 40% fine ice particles or snow of the total moisture by weight in a 5-gallon bucket. Then the slurry was poured into a 50-gallon barrel and frozen in a cold room at a temperature around 14 ^{o}F (-10 ^{o}C). The major reason for adding fine ice particles or snow was to prevent possible non-homogeneity of soil caused by particle settling during the freezing process. Adding ice or snow into the mixture also helped cool down the slurry and reduce the time for slurry freezing. Three moisture contents for the test silt (e.g., 50%, 80%, and 120% by weight) were prepared. These samples were used to investigate the effects of the moisture content on anchor behavior.

Figure 3.1 shows the materials used to form the slurry. The dry silt was a sublimated silt that had fallen on the permafrost tunnel floor in the Cold Regions Research and

Figure 3.1 Materials for remolding ice-rich silt.

Engineering Laboratory. The silt contained about 5~10% of organic materials by weight and less than 5% of sand with size between sieve NO.100 and NO.40. The plastic limit and liquid limit for the silt was about 34% and 38%, respectively (Zhu and Carbee, 1987; Bray, 2008). The specific gravity of the silt was about 2.68.

3.2 Laboratory Creep Test Setup

The laboratory test equipment was built to perform anchor load tests. Figure 3.2 showed a typical equipment setup. The system included a test anchor, a load frame and the data acquisition system. In this study, three such test setups as shown in Figure 3.2 were built. Detailed building and installing information was given in Appendix A. The test anchor was about 4 inches in diameter and 24 inches in length. The length-to-diameter ratio of test anchors was around 6, which was a little greater than that used in the literature (e.g., Vialov, 1959; Parmeswaan, 1981). The test anchor

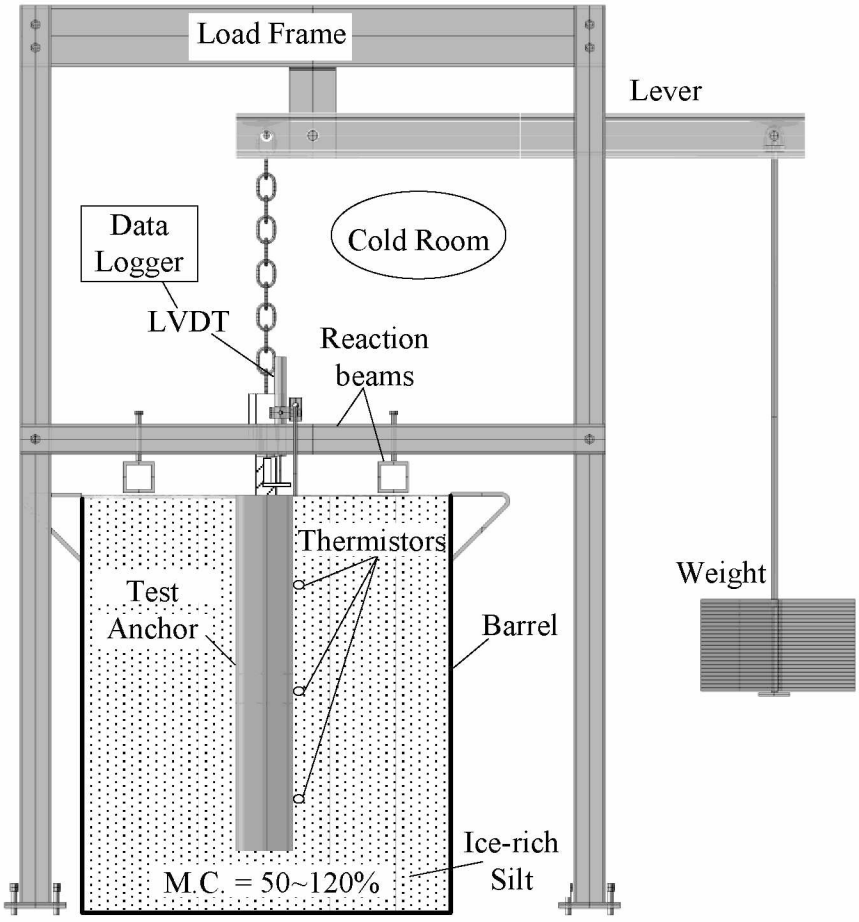

Figure 3.2 Anchor load test setup.

was embedded in remolded, ice-rich silt in a 50-gallon barrel and was loaded by a load frame. Constant loads were applied through a lever system and steel weights as shown in Figure 3.2. The load capacity of the frame was about 6.5 kips (29 kN). A Linear Variable Differential Transducer (LVDT) with an accuracy of 0.001 inch was installed to monitor anchor displacement. Several thermistors were installed along the anchor at different depths to monitor soil temperatures.

3.3 Anchor Installation Methods

Two methods were tried to install test anchors in ice-rich silt. In the first method as shown in Figure 3.3, an anchor was first placed at the center of a barrel and then the annular space was filled with remolded ice-rich silt layer by layer. Each layer of silt was up to 4 inches and compacted by a hand trowel. Sufficient time was allowed for the previous soil layer to freeze before placing the next layer of silt. After the anchor was fully embedded in the barrel, a constant-load creep test was performed, using the test setup described in Section 3.2. The test result indicated the pullout capacity of the anchor was about 700 lbs (shear stress = 2.3 psi) at a soil temperature of 30.2 ^{o}F (-1 ^{o}C). This method was not used in the rest of the laboratory tests since the installation method could not simulate the field installation process.

Figure 3.3 Install an anchor by layer silt placement and compaction.

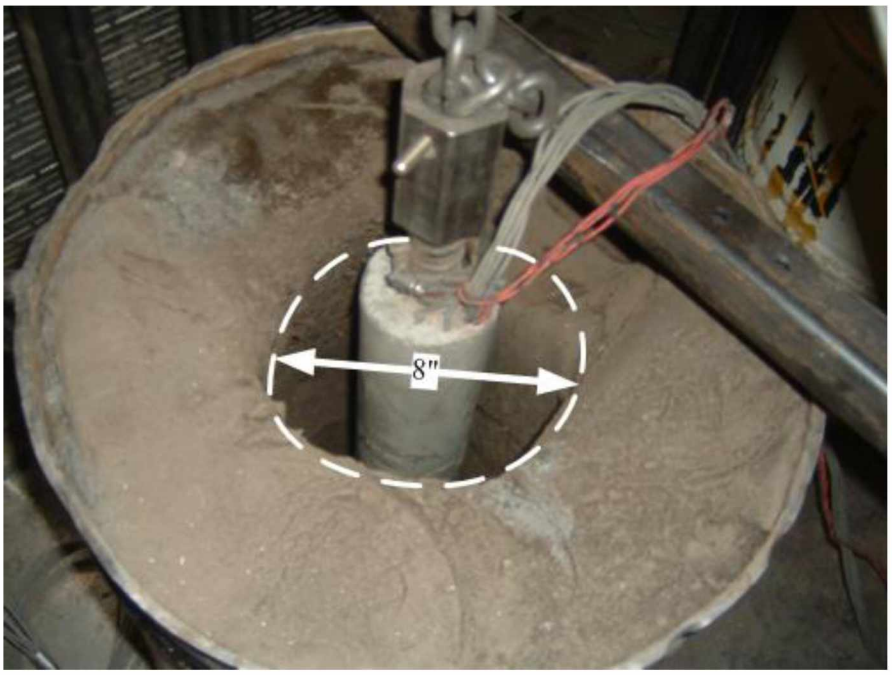

Figure 3.4 Install an anchor in a small annular space.

Figure 3.4 shows the second method used to install a test anchor in ice-rich silt. It involved first drilling an 8-inch-diamter hole in the ice-rich silt (see Appendix A for the procedure of hole making), and then placing the anchor inside the hole, and filling quickly the annular space with ice-rich silt slurry. After the slurry was frozen, a constant-load creep test was conducted. The trial test was performed at a constant temperature of 30.2 ^{o}F (–1 ^{o}C) in which three-staged loads were applied: 900 lb, 1500 lb, and 3000 lb. The anchor survived through the first two load stages (900 lb and 1500 lb) but failed at the third load stage (3000 lb). The failure stress obtained form the anchors installed by the two methods were 2.3 and 10 psi, respectively. This might be attributed to an increase in the confining stress caused by volume expansion of backfill soil slurry during freezing. It was considered that the second installation method can better simulate the field installation process and was adopted in this study.

3.4 Testing Procedures

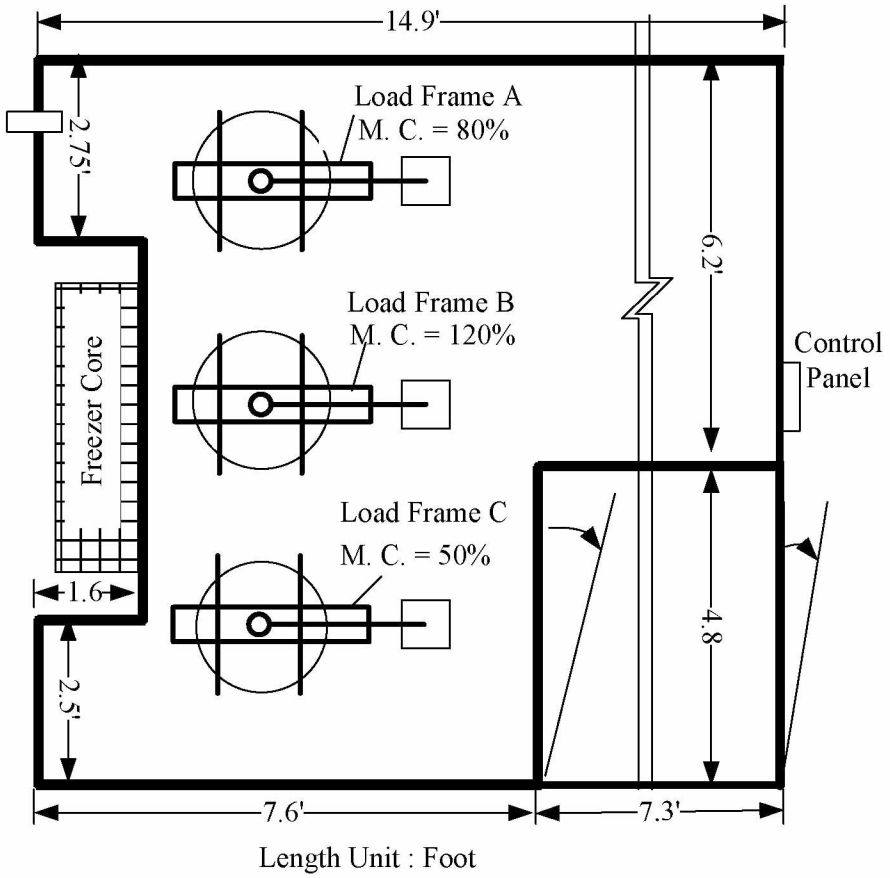

Figure 3.5 Layout of test equipment in the cold room.

All the creep tests were performed in the cold room at the Department of Civil and Environmental Engineering at University of Alaska Fairbanks. Figure 3.5 shows that layout of the equipment for the creep tests in the cold room in which the environment temperature was carefully controlled. Three anchor load tests (stage-loaded) were conducted concurrently by three test setups with three moisture content conditions. The testing procedures were as follows (detailed procedures were given in Appendix A):

1. Install the test anchor in a drilled hole;
2. Freeze the backfill soil slurry at a temperature of 14 ^{o}F (-10 ^{o}C) for about 2 days;
3. Condition the frozen silt at a designated constant temperature (e.g., 30.2 ^{o}F, 28.4 ^{o}F) for at least 4 days; and
4. Apply constant loads in stages by adding steel weights. The anchors were loaded in stages until a tertiary creep occurred or the capacity of load frame was reached. The anchor displacement was measured every 10 seconds during the loading period with a Campbell Scientific CR9000x data logger. Soil temperatures were recorded at each loading stage by reading thermistors with a multi-meter.

3.5 Test Results

A total of nineteen anchor load tests were conducted using the test method described above. Creep curves were obtained for different load stages, soil temperatures and soil moisture conditions. Examples of these results are given below. Detailed results are given in Appendix B.

Figure 3.6 shows five displacement vs. time curves obtained from Test # 3-120, in which the ice-rich silt with a water content of 120% was used. Each curve was obtained from a constant load stage under a constant temperature or temperature range. The temperature range represented the temperature distribution along the test anchor. Generally, all three creep stages as described in the literature review were observed. At low shear stresses (e.g., curve a, b, and c in Figure.3.6 with τ = 5.3~9.3 psi), the creep curve was characterized by rapidly decreasing displacement rate, which

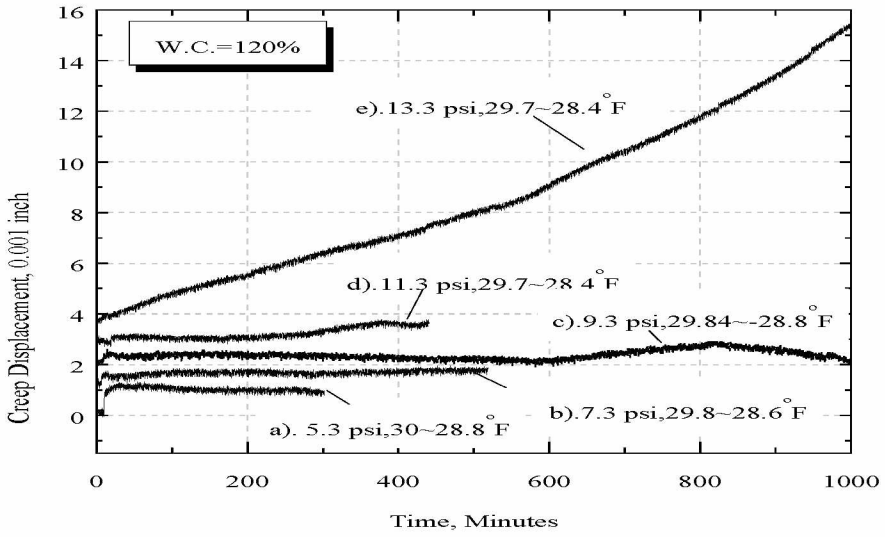

Figure 3.6 Example of the creep curves. (Test # 3-120).

corresponded to the primary creep. The creep curve at a higher shear stress of 11.3 psi (curve d in Figure 3.6) showed an approximate secondary creep stage in which the displacement rate was constant. At the highest shear stress of 13.3 psi (curve e in Figure 3.6), a well-defined secondary creep took place and followed by a tertiary creep with accelerated displacement rate.

To find the minimum creep displacement rate relationship, load stages that reached the secondary creep were identified and the corresponding displacement rates were determined approximately by the slope of creep curves. Figure 3.7 shows an example for estimating the displacement rate during the secondary creep stage. The linear portion of displacement curve was interpreted as the range of secondary creep. The

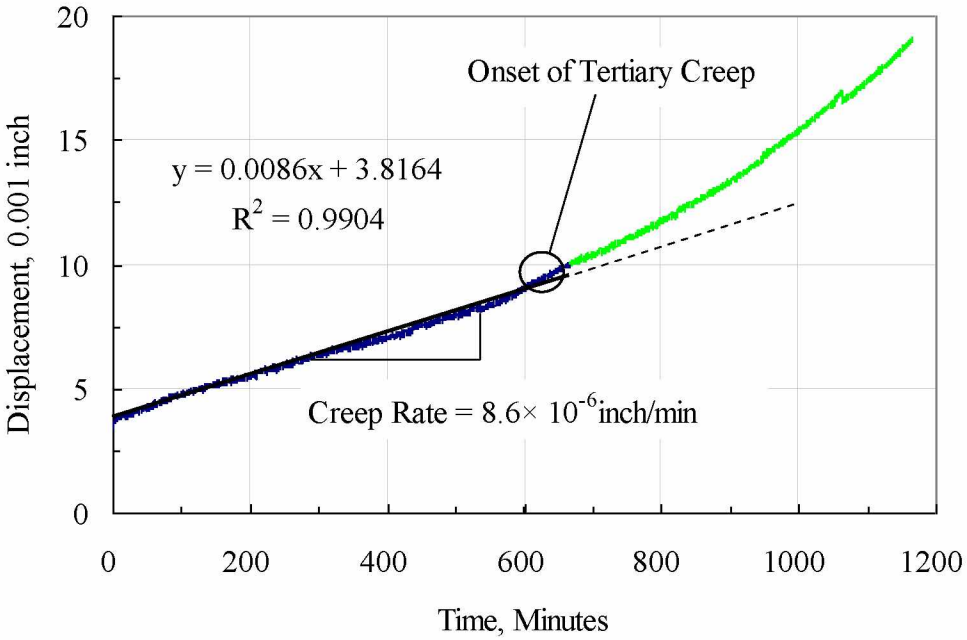

Figure 3.7 Determination of the displacement rate. (Test # 3-120, 13.3 psi)

end of the linear portion was interpreted as onset of the tertiary creep. Displacement limit for onset of the tertiary creep was about 0.01 inch in the example and usually less than 0.05 inch in the other tests. The values were much smaller than 1 inch which was suggested by Johnston and Ladanyi (1972) for rough anchors.

Figure 3.8 shows pictures of a test anchor subject to staged loads before and after failure. The displacement of surrounding silt at anchor failure was too small (less than 0.05 inches) to be observed. The shear strength of frozen soil, because of the limited deformation of the surrounding soil, might not have been fully developed. This agreed with the literature involving creep for smooth steel or concrete piles in frozen soil.

(a) (b)

Figure 3.8 Pullout failure pattern. (a) anchor before loading; (b) anchor after failure.

Usually the displacement rated was normalized to eliminate the influence of anchor diameter. The normalized displacement rate ($\dot{u}_a$ /a), which was defined as the displacement rate divided by the anchor radius (a=2 inch here), had a unit of inch/inch/year, or year^{-1}. Table 3.1 summarized the normalized displacement rates and the corresponding shear stresses and average soil temperatures obtained from this research. The results indicated that the occurrence of tertiary creep was usually associated with a high normalized displacement rate (e.g, from 0.7 to 215 year^{-1}). For those loads with normalized displacement rates below 0.7 year^{-1}, tertiary creep was not observed. Thus normal displacement rate at order of 0.7 year^{-1} may be considered as criteria for use in the design.

Table 3.1 Summary of displacement rates.

M.C.	T, °F (°C)	τ, psi	$\dot{u}_a / a$ year^{-1}	Tertiary creep occurred?
50%	31.3 (-0.4)	5.0	2.996	Yes
50%	30.7 (-0.7)	9.5	2.497	Yes
50%	29.8 (-1.2)	16.4	2.628	Yes
50%	29.5 (-1.4)	13.2	0.946	Yes
50%	27.9 (-2.3)	18.4	0.263	No
80%	31.3 (-0.4)	7.0	68.328	Yes
80%	30.9 (-0.6)	4.8	6.570	Yes
80%	30.7 (-0.7)	9.2	3.154	Yes
80%	30.6 (-0.8)	3.0	0.158	No
80%	29.8 (-1.2)	5.5	0.289	No
80%	29.8 (-1.2)	10.3	1.761	Yes
80%	29.7 (-1.3)	11.8	0.762	Yes
80%	29.7 (-1.3)	8.0	0.263	No
120%	31.8 (-0.1)	3.0	215.496	Yes
120%	31.3 (-0.4)	5.0	5.782	Yes
120%	30.6 (-0.8)	10.0	19.710	Yes
120%	30.6 (-0.8)	5.0	0.263	No
120%	30.2 (-1.0)	6.8	1.314	No
120%	30.2 (-1.0)	10.1	39.420	Yes
120%	29.5 (-1.4)	5.0	0.263	No
120%	29.5 (-1.4)	7.0	0.263	No
120%	29.5 (-1.4)	9.2	1.577	No
120%	29.5 (-1.4)	11.2	3.942	Yes
120%	29.1 (-1.6)	11.3	0.420	No
120%	29.1 (-1.6)	13.3	2.547	Yes
120%	29.8 (-1.2)	3.0	0.184	No

Note: M.C. is gravimetric moisture content of ice-rich silt; T is temperature; τ is applied shear stress; $\dot{u}_a / a$ is normalized displacement rate.

Chapter 4 Data Analysis and Discussion

4.1 Comparison with Rough Anchors Based on the Design Guidelines

The existing design guideline suggests using Equation 2.10 to design creep displacement of rough piles or anchors in permafrost (Morgenstern et al., 1980). Table 4.1 compared the normalized displacement rates for smooth anchors in this study with those for rough piles or anchors. At the same shear stresses, the measured displacement rate is much greater than those given by Equation 2.10. Thus, Equation 2.10 should not be used for smooth anchors because of safety consideration, even though it was considered conservative for rough piles or anchors in ice-rich soils.

Table 4.1 Test results versus prediction by the existing design guidelines. (Symbols were defined before in Table 3.1).

T, °F (°C)	M.C.	τ, psi	Measured $\dot{u}_a$ /a year^{-1}	Predicted $\dot{u}_a$ /a year^{-1}	Comments
(-1.2)	50%	16.4	2.628	0.130~0.292	The upper limit of predicted displacement rate is based on temperature of 30.2 °F and lower limit 28.4 °F.
(-1.4)	50%	15.8	94.608	0.116~0.261	
(-1.2)	80%	5.5	0.289	0.004~0.011	
(-1.2)	80%	10.3	1.761	0.032~0.072	
(-1.3)	80%	11.8	0.762	0.048~0.109	
(-1.3)	80%	8.0	0.263	0.015~0.033	
(-1.0)	120%	6.8	1.314	0.009~0.020	
(-1.0)	120%	10.1	39.420	0.030~0.068	
(-1.4)	120%	5.0	0.263	0.003~0.008	
(-1.4)	120%	7.0	0.263	0.010~0.022	
(-1.4)	120%	9.2	1.577	0.022~0.051	
(-1.4)	120%	11.2	3.942	0.041~0.093	
(-1.6)	120%	11.3	0.420	0.042~0.095	
(-1.6)	120%	13.3	2.547	0.069~0.156	
(-1.2)	120%	3.0	0.184	0.000~0.001	

4.2 Development of a Time-Dependent Creep Equations

Because the existing design guidelines were not applicable to our cases, a new creep equation then needed to be developed to describe the creep of smooth anchors in ice-rich silt. In this study, the equation used for determining the regression of the test data was:

$$\tau_f = \tau_m \theta^b \left(\frac{\dot{u}_a}{a} \right)^{1/n} \tag{4.1}$$

where n is the stress exponent, τ_f the measured failure shear stress, or ultimate shear stress, τ_m the general creep modulus, b the temperature exponent, and θ the degrees of temperature below freezing point (32 ^{o}F). Equation 4.1 was essentially analogues to Equation 2.12. Similarly, the stress exponent, n, was considered independent of the temperatures. The Equation 4.1 assumed that the ultimate shear stress is dependent on the displacement rate.

Equation 4.1 was used to model the test data with different soil moisture contents (see Table 3.1). A Least-Square regression approach was employed and the results are shown in Table 4.2. The stress component, n, was greater than those suggested in the design guidelines (n=3) and varied with soil moisture content. The creep modulus, τ_m, increased as soil moisture content was reduced. For different soil moisture contents, there was a slight difference between the temperature exponent, b.

Table 4.2 Summary of the regression analysis. (Soil temperatures from 0~-2.5 °C).

Moisture Content	τ_m(psi)	b	n	R^2	S_E (psi)
120%	4.0	0.86	6.07	0.78	1.7
80%	3.7	1.27	3.90	0.67	2.0
50%	5.5	1.07	3.91	0.98	1.2

Note: S_E is Standard Error of Estimate.

The Standard Error of Estimate (S_E) is provided in Table 4.2. Then a lower 97.5% limit of the shear stress can be computed as:

$$\tau_f = \tau_m \theta^b \left(\frac{\dot{u}_a}{a} \right)^{1/n} - 2S_E \tag{4.2}$$

For practical design, a safety factor (FS) may be applied to Equation 4.2 and the allowable shear stress can be determined as:

$$\tau_{a,all} = \frac{\tau_m \theta^b \left(\frac{\dot{u}_a}{a} \right)^{1/n} - 2S_E}{FS} \tag{4.3}$$

In the literature, a safety factor of 2.0~3.0 was suggested for piles in permafrost. An appropriate safety factor in Equation 4.3 should be based on filed consideration. Thus, additional test data might be required by conducting anchor load tests in the field.

4.3 Effect of Soil Moisture Content and Temperature

The relationship between shear stresses and displacement rates is shown in Figure 4.1 for different soil moisture contents. The plot was based on Equation 4.1 and the

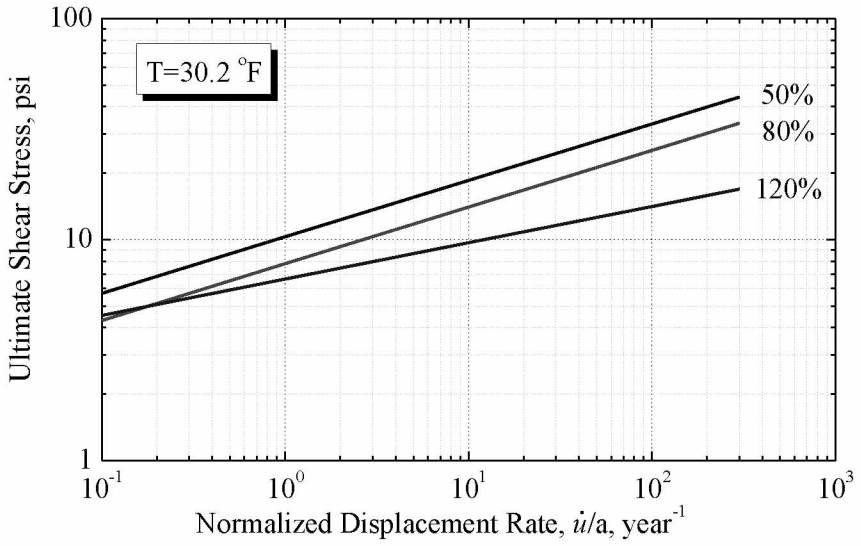

Figure 4.1 Effects of soil moisture contents on anchor creep.

parameters in Table 4.2 and considered only one soil temperature of 30.2 °F. It was found that creep displacement rates increased with the increasing of soil moisture content. As indicated in the literature, piles or anchors in ice exhibits greater creep displacement or displacement rate than in ice-rich soil. Thus, the finding in this study was consistent with the existing literature. Especially, the regression equations in this study provided a way to evaluate quantitatively the effects of moisture content. The finding was also applicable to the testing range of normalized displacement rate between 0.2 and 300 $year^{-1}$, and to other soil temperatures (e.g., 28.4 or 27.5 °F).

Figure 4.2 shows the effects of soil temperature on the creep behavior of grouted anchors in ice-rich silt with the same moisture contents. Creep displacement rates decreased as the soil temperature reduced, which was consistent with findings

reported by other researchers for other soil moisture. Thus, great care should be taken to design grouted anchors in warm ice-rich soil.

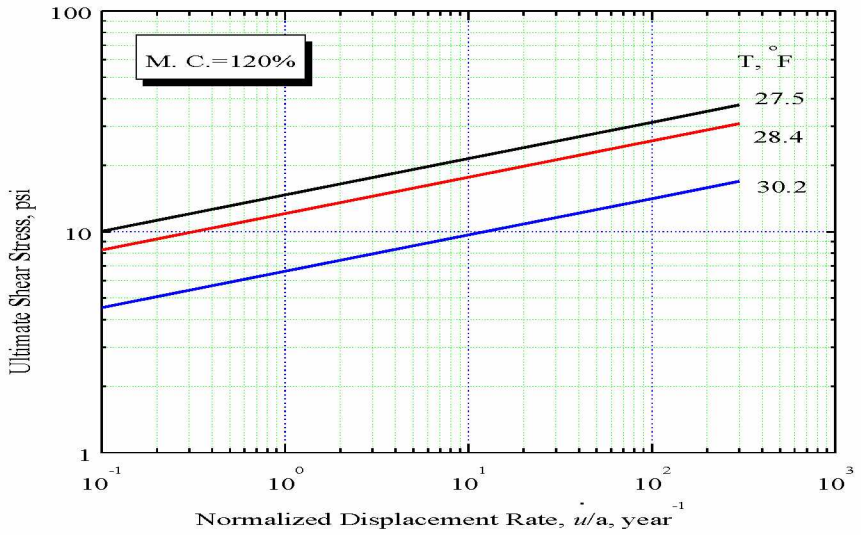

Figure 4.2 Effects of soil temperatures on anchor creep. (M.C. =120%).

4.4 Design Example

A new creep equation was proposed in this study for creep design of smooth anchors in ice-rich silt. An example of using the equation in anchor design was given below.

Example 4-1: A 2-inch-radius anchor is embedded in ice-rich silt. The anchor embedment of anchor is assumed to be 10 ft. The ice-rich silt has a temperature of 28.4 ^{o}F (-2 ^{o}C) and a moisture content of 80%. Consider the following problems:

1. Evaluate the anchor creep displacement rate by Equation 4.3, if an allowable shear stress of 14.5 psi is chosen. The allowable shear stress is based on the ultimate adfreeze strength for concrete piles in silt slurry and a safety factor of 2.5

(TM-5-852-4/AFM 88-19, Chap. 4, 1983).

2. Determine the allowable pullout capacity so that the creep displacement rate does not exceed 0.2 inch per year and the shear stress does not exceed the allowable shear stress of 14.5 psi.

Solution:

1. Creep equation for the silt with moisture content of 80% at a shear stress of 14.5 psi is (from Equation 4.3 and Table 4.2):

$$\tau_{a,all} = \frac{3.7\theta^{1.27}\left(\frac{\dot{u}_a}{a}\right)^{1/3.90} - 2\times 2.0}{FS}$$

or $$\frac{\dot{u}_a}{2} = \left[\frac{(2.5\times 14.5 + 2\times 2.0)}{4.0}\times\frac{1}{(32-28.4)^{1.27}}\right]^{3.90} = 14.3 \text{ year}^{-1}$$

or $$\dot{u}_a = 2\times\left[\frac{(40.25)}{4.0}\frac{1}{(3.6)^{1.27}}\right]^{3.90} = 28.6 \text{ inch/year}$$

The normalized displacement rate, 14.3 year^{-1}, is within the testing range (0.2 ~ 300 year^{-1}).

2. The shear stress which limits the creep displacement rate to 0.2 per year can be calculated as:

$$\tau_{a,all} = \frac{3.7\theta^{1.27}\left(\frac{\dot{u}_a}{a}\right)^{1/3.90} - 2\times 2.0}{FS}$$

or $$\tau_{a,all} = \frac{3.7\times 3.6^{1.27}\times\left(\frac{0.2/1}{2.0}\right)^{1/3.90} - 2\times 2.0}{2.5} = 2.6 \text{ psi, which is smaller than}$$

the allowable shear stress of 14.5 psi given in the literature. The allowable pullout capacity, P_{all}, is computed as:

$$P_{all} = 2\pi aL\tau = 2 \times \pi \times 2 \times (10 \times 12) \times 2.8 = 4222 \text{ lbf or } 4.2 \text{ kips}$$

4.5 Design Charts

Based on the regression results, tentative design charts were developed for three moisture conditions for ice-rich silt. The curves are given in Figure 4.3 to Figure 4.5. The allowable shear stresses were calculated based on Equation 4.3 and Table 4.2. The displacement rates were selected to represent the testing range which was from 0.2 to 300 year^{-1}. As shown in the Example 4-1, the allowable shear stress for a low displacement rate was smaller than those given in the literature (TM-5-852-4/AFM 88-19, Chap. 4, 1983).

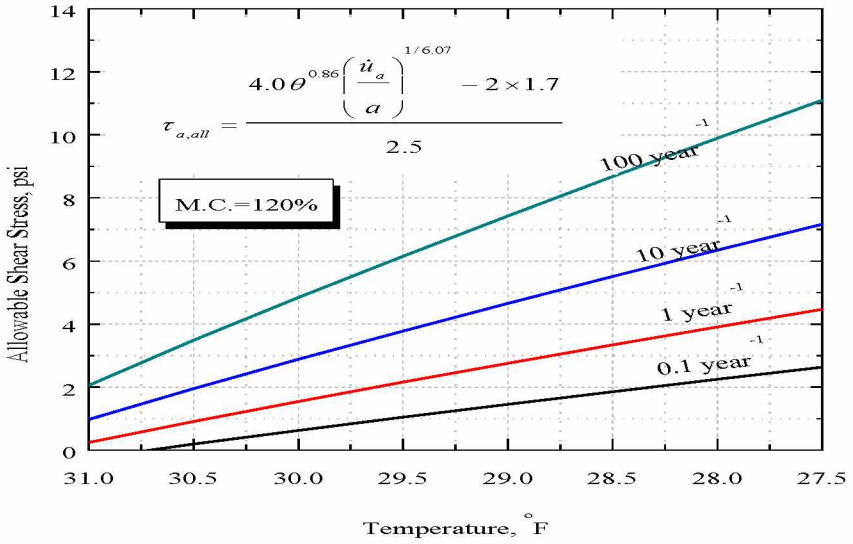

Figure 4.3 Tentative design chart for ice-rich silt with M. C. = 120%.

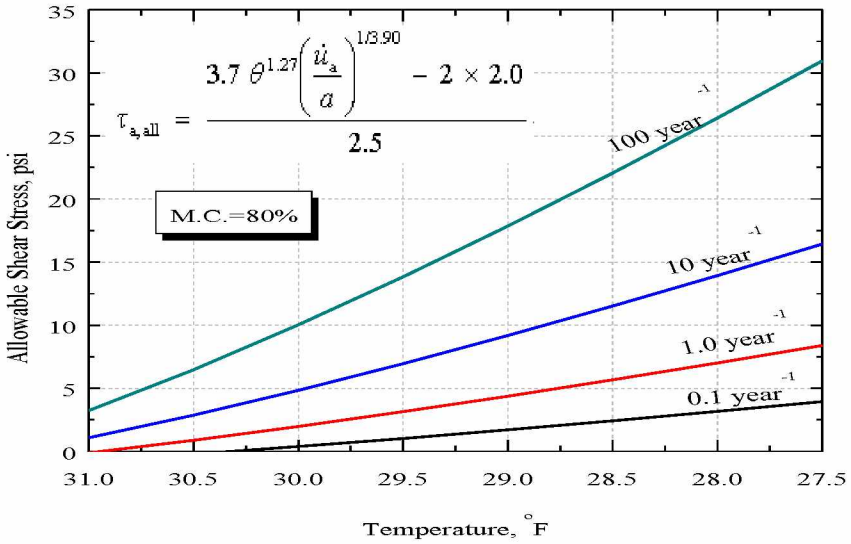

Figure 4.4 Tentative design chart for ice-rich silt with M. C. = 80%.

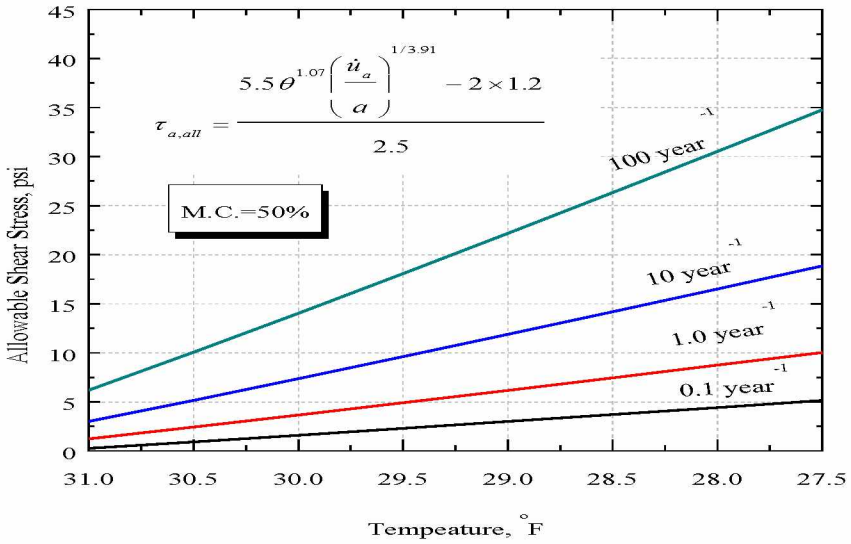

Figure 4.5 Tentative design chart for ice-rich silt with M. C. = 50%.

Chapter 5 Conclusions and Recommendations

5.1 Conclusions

The major findings of this study were summarized as followings:

1. The existing design guidelines were not applicable to the test data obtained in our study. This is because of different anchor surface conditions. Higher creep displacement rate were observed for relatively smooth anchors in this study, compared to rough anchors given by the existing design guidelines.
2. It was recommended that the creep equation based on regression analysis of test data be used for smooth grouted anchors in ice-rich silt with temperatures from 0 to -2.5 ^{o}C. The normalized displacement rate in the equations typically ranged from 0.2 to 300 year^{-1}.
3. The regression equation indicated that the displacement rate increased with an increase of soil moisture contents and soil temperature. This conclusion was consistent with the existing literature.
4. The displacement limit for onset of tertiary creep for smooth grouted anchors in ice-rich silt is close to 1 mm. Limited displacement for slip indicated that shear strength of the frozen silt may not have been fully developed. This finding agrees with the literature associated with smooth steel piles.
5. Great care must be taken when working with smooth anchors in ice rich silt for temperature range of 32 ^{o}F to 28.4 ^{o}F, as the allowable shear stresses were much lower than those for rough piles.

5.2 Recommendations

1. Creep behavior of grouted anchors with smooth surface configurations was investigated in this study. Since the anchors grouted in the field usually have rough surface, it is suggested that field anchor load tests be performed to examine the influence of other surface configurations on the creep behavior of grouted anchors.
2. The lengths and diameters of the test anchors were constant in this study. Future research needs to examine the influence of the anchor length and diameter on the creep behavior.
3. This study focused on the creep behavior of grouted anchors in ice-rich silt. The findings from this research might not applicable for grouted anchor in other soil types, such as ice-rich sand or clay. More research is needed in this direction.
4. Effects of the moisture content were investigated for the creep of grouted anchors in this study. It was found that the displacement rate increased with an increase in the soil moisture content. This effect might be related to the unfrozen water content and the ice distribution with the embedment depth. More research is needed in this direction.

References

Andersland, O. B., and Ladanyi, B. (2004). *Frozen ground engineering,* Second edition. American Society of Civil Engineers & John Wiley & Sons, Inc, Hoboken, New Jersey.

Biggar, K. W., and Sego, D. C. (1990). "Field load testing of various pile configurations in saline permafrost and seasonally frozen rock." *Proceedings, 42nd Canadian Geotechnical Conference*, October 24-27, Winnipeg: 304-312

Biggar, K. W. 1991. Adfreeze and grouted piles in saline permafrost. *Ph. D. Thesis*, University of Alberta, Canada: 449 pp.

Biggar, K. W., and Sego, D. C. (1993a). "Field pile load tests in saline permafrost." I. Test procedures and results. *Can. Geotech. J.* Vol.30 (1): 34-45

Biggar, K. W., and Sego, D. C. (1993b). "The strength and deformation behavior of model adfreeze and grouted piles in saline frozen." *Can. Geotech. J.* Vol.30: 319-337

Biggar, K.W., and Sego, D.C. (1994). "Time-dependent displacement behaviour of model adfreeze and grouted piles in saline frozen soils." *Can. Geotech. J.* Vol. 31: 395–406.

Biggar, K. W., and Kong, V. (2001). "An analysis of long-term pile load tests in permafrost from the Short Range Radar site." *Can. Geotech. J.* Vol. 38: 441-460

Bray, M. T. 2008. "The influence of soil crystructure on the creep and long term strength properties of frozen soils." *Ph.D. Thesis*, Univerisity of Alaska Fairbanks.

Johnston, G. H., and Ladanyi, B. (1972). "Field tests of grouted rod anchors in permafrost." *Can. Geotech. J.*, Vol.9: 176-194

Johnston, G. H., Ladanyi, B. (1974). "Field tests of deep power-installed screw anchors in permafrost." *Can. Geotech. J.*, Vol.11: 348-358

Linell, K. A. and Lobacz, E. F. (1980). "Design and construction of foundation in areas of deep seasonal frost and permafrost." *Special Report*, U.S. Army Cold Regions Research and Engineering Laboratory: 80-34. P:320

Ladanyi, B. (1972). "An Engineering theory of creep of frozen soils." *Can. Geotech. J.*, Vol.9 (1): 63-80

Ladanyi, B. (1988). "Short- and Long-term behavior of axially loaded bored piles in permafrost." *Deep Foundations on Bored and Auger Piles*, Van Impe(ed.) Balkema, Rotterdam, pp. 121-130.

Morgenstern, N. R., Roggensack, W.D., and Weaver, J. S. (1980). "The behavior of friction piles in ice and ice-rich soils." *Can. Geotech. J.*, Vol.17:405-415

Morgenstern, N. R. and Sego, D.C. (1981). "Performance of temporary tie-backs under winter conditions." *Can. Geotech. J.*, Vol.18:566-572

Nixon, J.F., and McRoberts, E.C. (1976). "A design approach for pile foundations in permafrost regions". *Can. Geotech. J.*, Vol.13:40-57

Nixon, J.F., and Neukirchner, R. J. (1984). "Design of vertical and laterally loaded piles in saline permafrost." *Proceedings, 3rd International Specialty Conference on Cold Regions Engineering*, Edmonton, Alberta, Canadian Society of Civil Engineering, 1-6 April, pp: 131-144

Nixon, J.F. (1988). "Pile load tests in a saline permafrost at Clyde River, Northwest Territories." *Can. Geotech. J.*, Vol.25:518-529

Parameswaran, V. R. (1978). "Adfreeze strength of frozen sand to model piles." *Can. Geotech. J.*, Vol.15 (4): 494-500

Parmeswaran, V. R. (1981). "Creep of model piles in frozen soil". *Can. Geotech. J.*, Vol.16 (1): 8-16

Parmeswaran, V. R. (1986). "Bearing Capacity Calculations for Piles in Permafrost". *Proceedings of the 4th International Conference Cold Regions Engineering*, TCCRE, ASCE, Anchorage, AK, February 24-26, p. 751 -759

Phukan, A. (1985). *Frozen Ground Engineering*. Prentice-Hall, Englewood Cliffs, N.J.

Powers, W. F., and Briaud, J.-L. (1993). "Behavior of 10 full scale ground anchors installed in stiff clay." *Res. Rep.* to Schnabel Found. and the Fed. Hwy. Admin., Dept. of Civ. Engrg., Texas A&M University, College Station, TX.

Sego D. C., and Biggar K. W. (1990). "Grouts for use in permafrost regions." *Geotechnical News*, 8 (3): 33-34

Stelzer, D., and O. B. Andersland. (1989). "Pile roughness and load capacity in frozen soils". *In Cold Regions Engineering: Proc. 5th Int. Conf Minneaplis*. New York: Technical Council for Cold Regions Engineering, ASCE, pp: 226-35

TM-5-852-4/AFM 88-19, Chap. 4 (1983). "Arctic and subarctic constructions for structures." *Technical manual*. Department of the Army and the Air Force.

Vialov, S. S. (1959). "Rheological properties and bearing capacity of frozen soils." *Transl.* 74, US. Army Cold Regions Research Engineering Lab, Hanover, New, Hampshire, p: 219

Vinson T. S. and McHattie, R. L. (2009). "Documenting best management practices for ice-rich soils and permafrost sites." *Summary rep.* to Alaska Department of Transportation and Public Facilities, Fairbanks, AK

Weaver, J. S. (1979). "Pile foundations in permafrost." *Ph.D. Thesis*, University of Alberta, Edmonton, Alta, p: 225.

Weaver, J.S., and. Morgenstern, N. R. (1981). "Pile design in permafrost." *Can. Geotech. J.* Vol.18 (3):357-370

Appendix A: Anchor Load Tests in the Laboratory

The purpose of Appendix A was to provide detailed information about the anchor load tests in the laboratory. Section A.1 described the anchor fabrications and configurations. Section A.2 described design of the load frames. Section A.3 described the method for displacement measurement. Section A.4 described the detailed testing procedures.

A.1 Test Anchor Configurations and Fabrications

The configuration of the test anchors is shown in Figure A.1. A typical anchor has a length of 24 inches, and a diameter of 4 inches. The thread bar provided by DYWIDAG Systems International (DSI) was used as the anchor tendon. The bar had a diameter of 1.375 inches, effective section area 1.58 in^2, yielding load 189kips, ultimate load 237 kips, and a unit weight 5.56 lb/ft. The section of the threaded bar facilitate the installation of strain gages at the flat sides. Thermistors were installed in order to monitor the temperature along the anchor embedment. Each thermistor was calibrated by a pure ice-water mixture which has a temperature of 0 ^{o}C. The resolution of the thermistors was ± 0.1 ^{o}C. Strain gages were also installed along the tendon with intention to monitor the strain distribution along the tendon. But most of them performed poorly after installation due to frequent transportation of anchors and accidental cable damage.

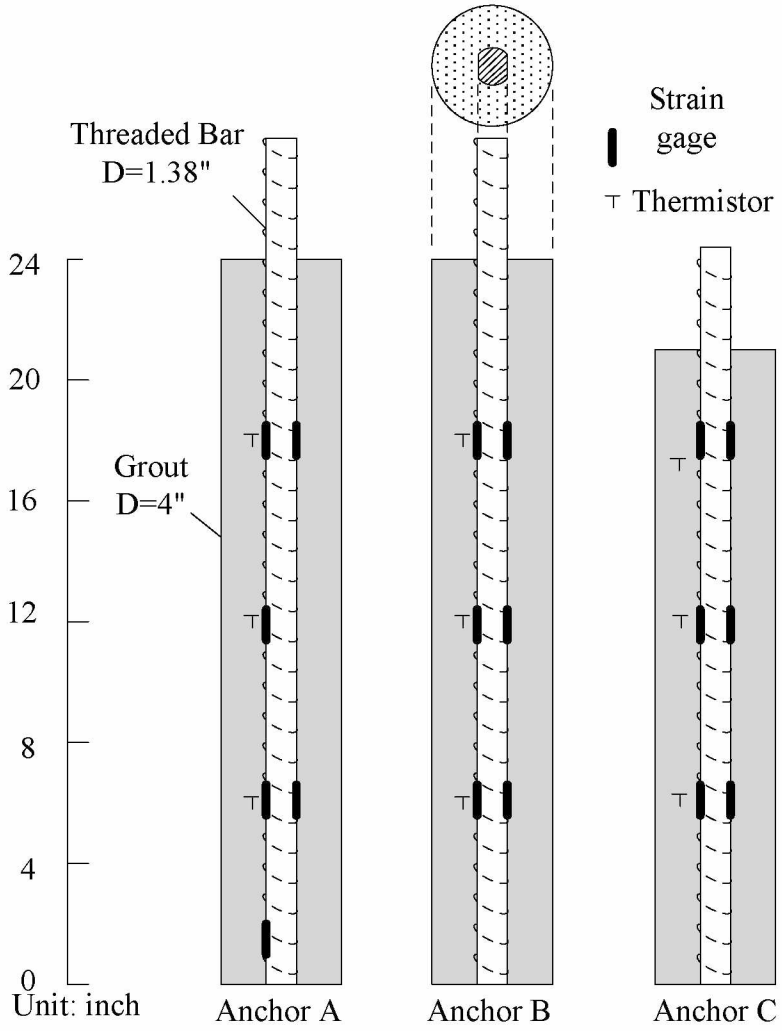

Figure A. 1 Configuration of the test anchors.

Figure A.2 shows the procedures of anchor fabrication. Plastic molds were made as the grout formwork. Non-Shrink Precision Grout purchased in the local store was hand mixed with water. According to the product specification, about 9.5 pints (20 liters) of water was added into 50 lbs grout materials to form a flowable mixture. The instrumented tendon was placed into the plastic mold and fixed at the center of the plastic mold. Then the fresh grout was poured into the annular space between the

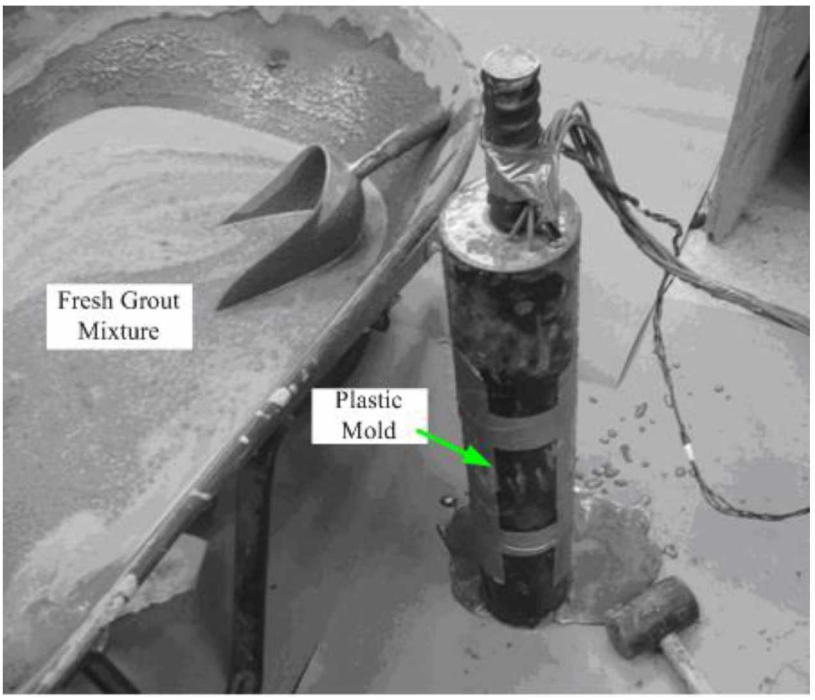

Figure A. 2 Fabrication of the test anchors.

tendon and the plastic mold. A rubber mallet was used to tamp the plastic model to facilitate the flow of the grouted materials.

Figure A.3 shows the three anchors made by above method. Generally, the anchors had a smooth lateral surface, except for some corrugated area due to the uneven inside surface of plastic mold. In this study, the newly grouted anchors were cured at a damp and warm place for three days. After three days, the plastic molds were removed and another four day's curing in the water was performed. The seven day's tension strength for the grout materials were tested by similar grout samples and were found to range from 480 psi to 626 psi. These values were acceptable, compared to a typical value of 420 psi for normal grout (Powers and Briaud, 1993).

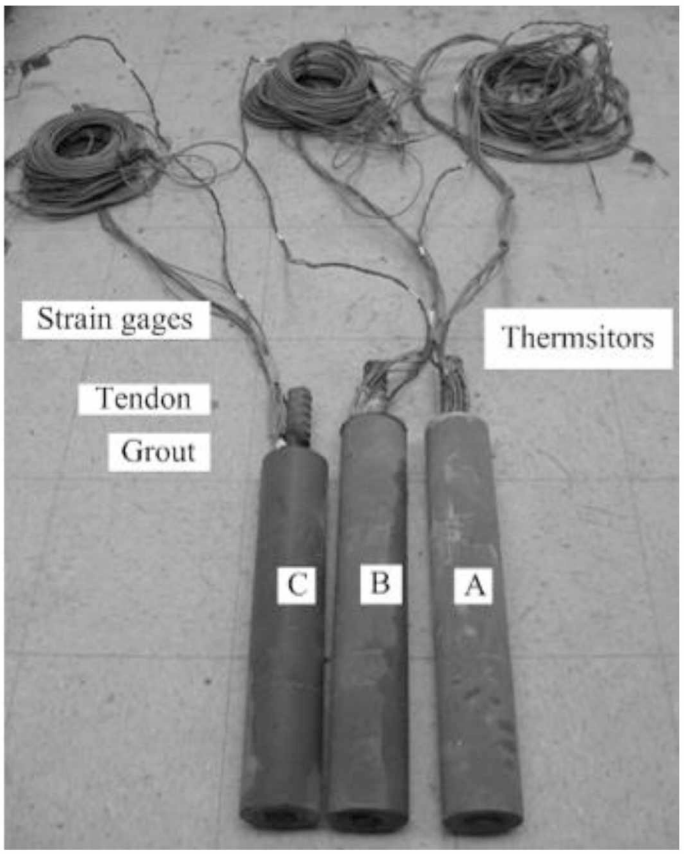

Figure A.3 Configuration of the test anchors.

A.2 Load Frame Configurations and Calibrations

Figure A.4 shows the dimensions of the load frame for anchor load tests. The load frame was 50 inches high and 50 inches wide, with the third direction about 4 inches. The frame consisted of one main box beam supported by four columns. A lever was made from two channel beams, with a lever arm ratio of 10. The lever was bolted to the main beam at a flat bar. At the rotation point of the lever, a needle bearing was used to reduce the friction. A steel chain was used to connect the short end of lever and the hex nut of the anchor head. Two beams were placed on the frozen soils together with the barrel and overlaid by another two beams which were connected to

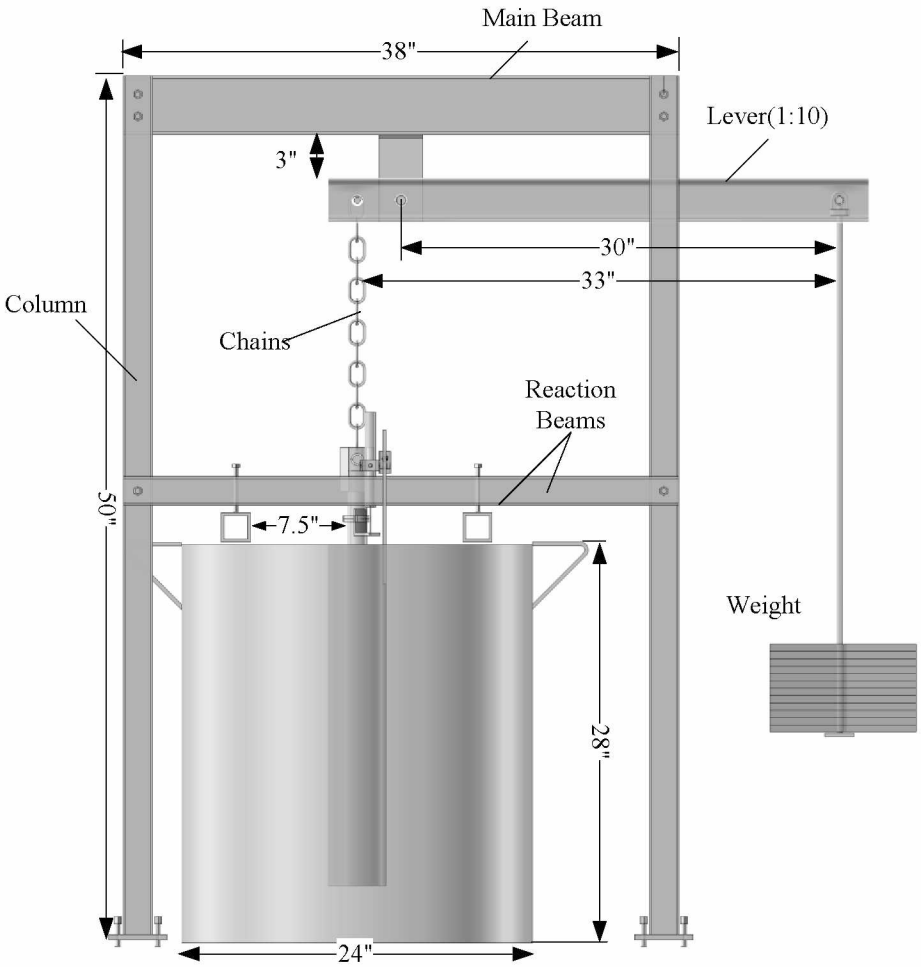

Figure A.4 Front view of the Load frame with dimensions.

the frame columns (see Figure A. 4). In this way, the movement of barrel was restrained. The design pullout capacity of the test frame was about 7 kips, corresponding to a shear stress on the anchor about 20 psi.

Figure A.5 provides a perspective view of the load frame. Figure A.6~A.8 show the sections of the principle elements in the load frame. And Table A.1 gives the section details of the principle frame elements.

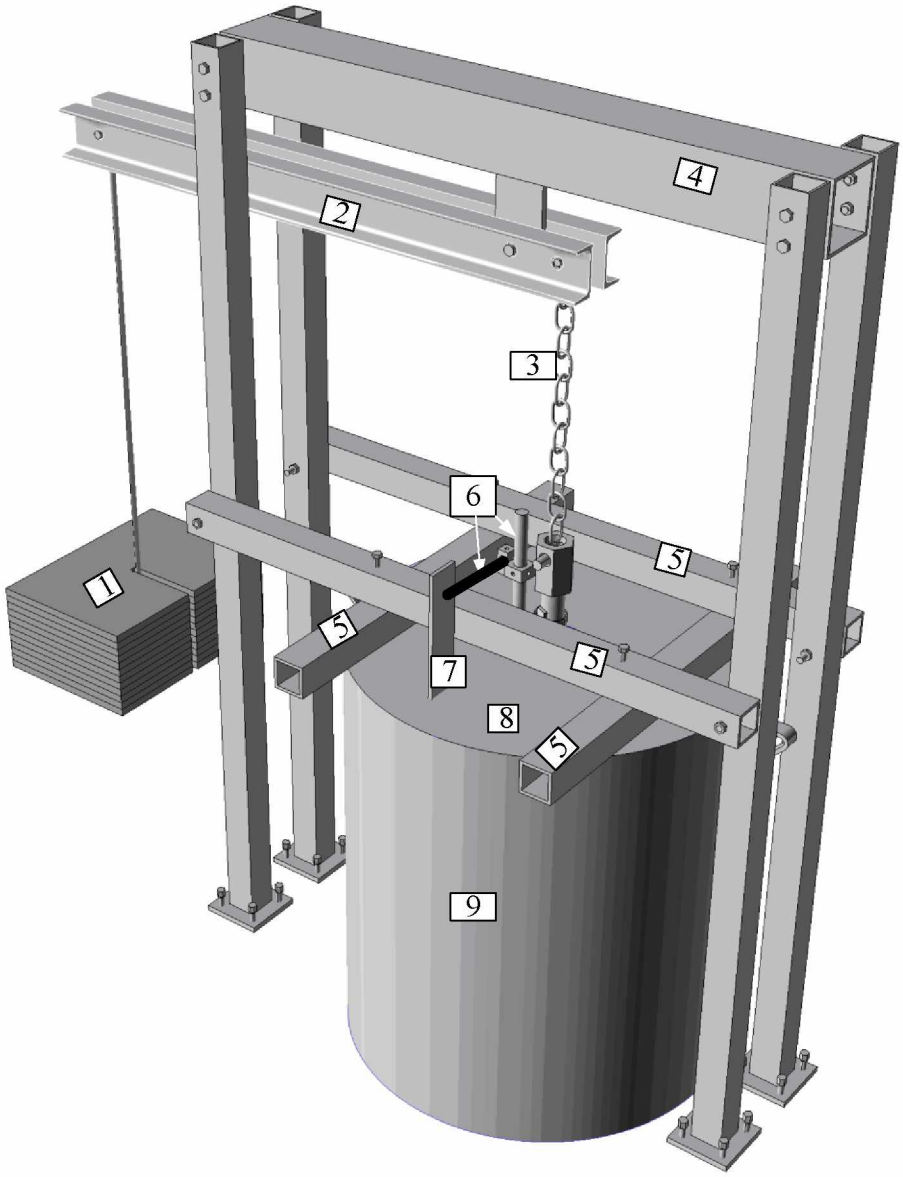

Figure A.5 Perspective view of the load frame. (1). Weights; (2). Lever arm; (3). Steel chain. (4). main beam; (5). Reaction beams; (6). LVDT stand; (7). Flat steel bar; (8). Frozen silt; (9) Barrel.

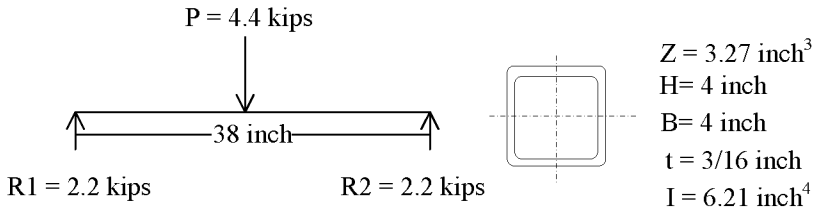

Figure A.6 Section of the main beam.

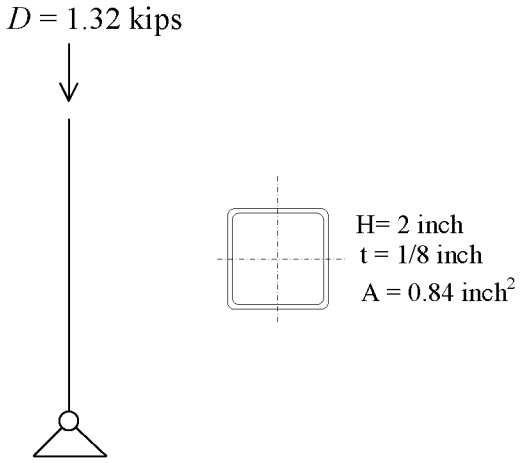

Figure A.7 Section of the column.

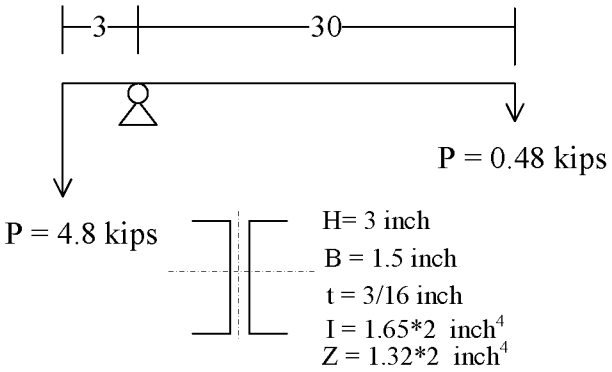

Figure A.8 Section of the column of lever

Table A. 1 Summary of the load frame elements.

Parts	Beam Type	Section (in)	Weight (lb/ft)	Length / Piece(in)
Main beam	Box Beam	4*2*1/4	8.80	38
Columns	Box Beam	2*2*1/8	3.04	50
Lever	Channel	4*2*1/8	4.75	36
Reaction beam	Box Beam	2*2*1/8	3.04	38

Figure A.9 to A.11 give the calibration curves for the lever arm. The arm ratio was calibrated by a load cell at both the room temperature and the cold temperature. Minor difference was found between these two temperatures. The load applied on the anchor was calculated based the calibrated ratio and the added steel weights.

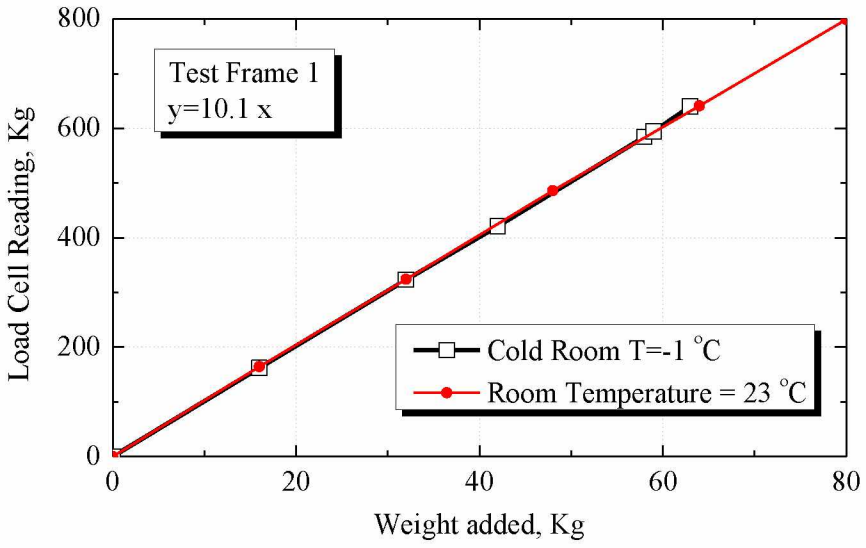

Figure A. 9 Calibration Curves for Test Frame 1.

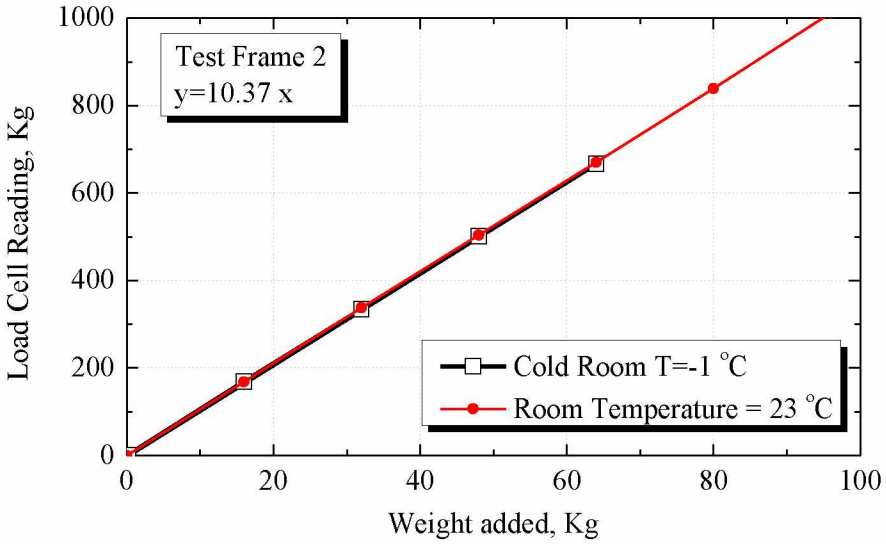

Figure A. 10 Calibration Curves for Test Frame 2

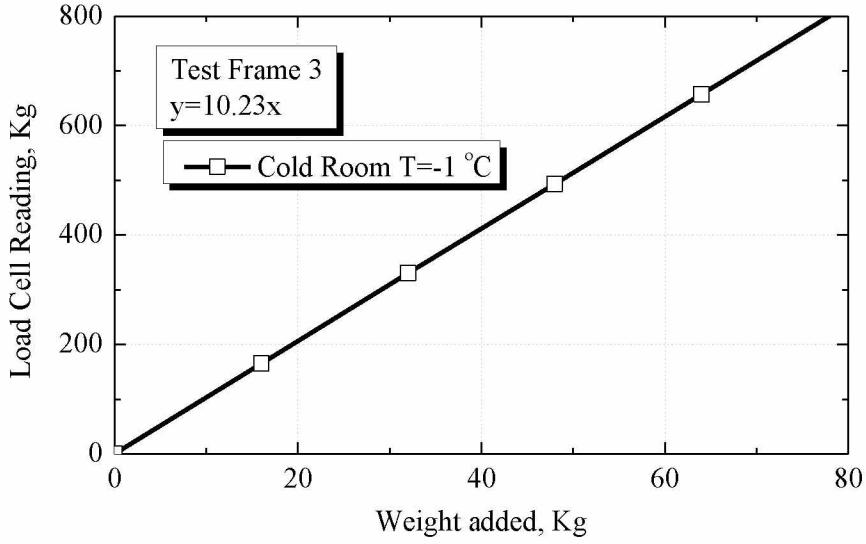

Figure A. 11 Calibration Curves for Test Frame 3.

A.3 Displacement Measurement

The relative movement between the anchor and surrounding soils was measured by a LVDT, as illustrated in Figure A.12. The LVDT had a thermal effect smaller than

0.003% and a resolution of ±0.001 inch after calibration (See Figure A.7). The working temperature for the LVDT ranged from -20 °C to 80 °C. In Figure 3.7, two reaction beams were hidden so that the LVDT and the mounting place can be seen. The LVDT was connected to a base on the anchor tendon and mounted on a flat steel bar with a magnetic LVDT holder. The flat steel bar was embedded about 4 inches into the frozen soils and was about 5 inches from the anchor. It was just out of the region covered by the reaction beams. The flat steel bar was free of forces. It was considered that the measurement was not affected by the movement of the oil drum or the deformation of test frame after loading.

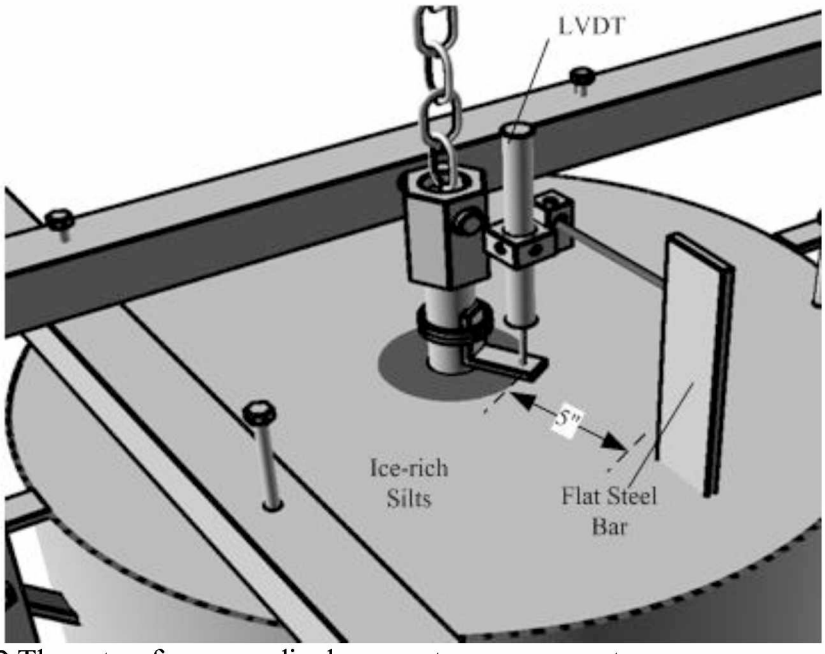

Figure A.12 The setup for creep displacement measurement.

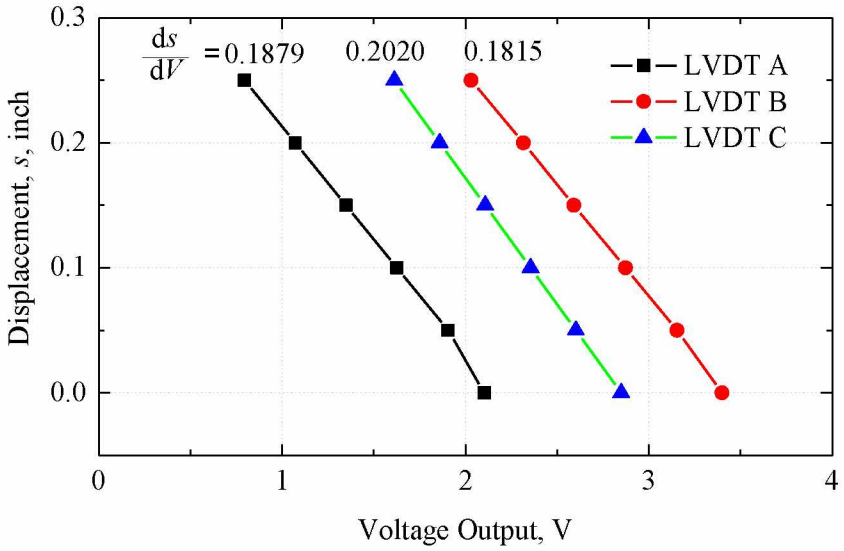

Figure A.13 Calibration Curves for the LVDT.

A.4 Testing Procedures

The detailed procedures to conduct an anchor load test in laboratory are given below.

1. Make an oversized hole.

Figure 3.9 illustrates process for making an oversized hole in the ice-rich silt stored in the barrel. There was an anchor embedded in silt which was failed in the previous test. The barrel was laid down firstly on a hand truck. Then a nozzle which was connected to the hot-water faucet could generate pressurized hot-water to wash the frozen silt around the anchor. Only the silt around the anchor was washed away. After the anchor was taken out, the hot-water circulation was continued to form a relatively round hole with a diameter about 8 inches. A basin below the barrel was used to collect the thawing silt so that the sink would not be filled and blocked. It took take about fifteen to thirty minutes to make such a hole. No significant thawing happened to the rest of

silt during this process.

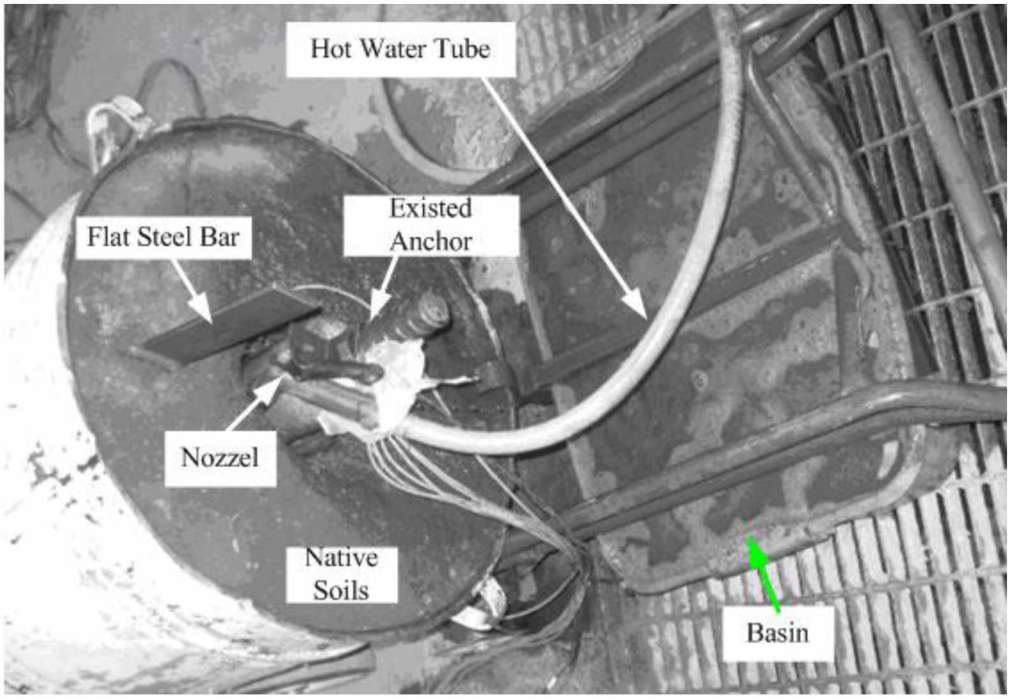

Figure A.14 Make an oversized hole by hot-water washing.

2. Backfill with ice-rich slurry

In Figure A.15, an anchor was placed at the center of the oversized hole made in the last step. Then the annular space was backfilled with ice-rich silt slurry. The slurry had the same moisture content as the native silt. A steel rod was used to stir the slurry after each round of backfilling. It took 3 to 4 placement to fill the whole the annular space. The freezing process was not started until the annular space was filled.

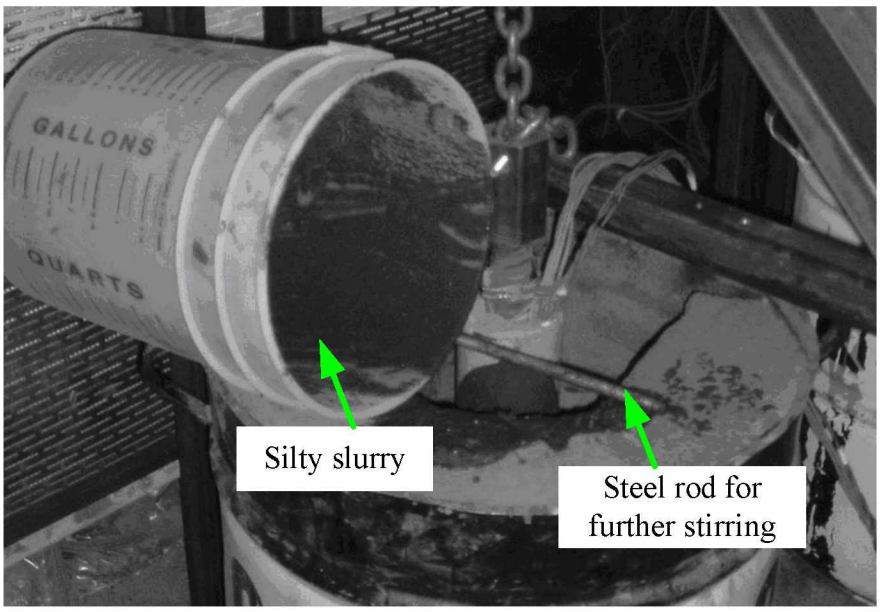

Figure A.15 Backfill the silt slurry into the annular space.

3. Slurry freezing and soil conditioning

Figure A.16 shows the test anchor embedded in the unfrozen silt slurry in the oversized hole. The slurry was frozen for two or three days. The temperature of the cold room was usually set to -10 ^{o}C for freezing. Massive ice was found on the surface during the freezing process.

Figure A.16 The test anchor embedded in the unfrozen silt.

Figure A.17 Ice formed on the surface after the silt was frozen.

4. Cable wiring and weight loading

After the freezing process finished, another 4 to 5 days were needed to condition the silt at the designated temperatures (e.g., -0.5 ^{o}C, -1.5 ^{o}C, and -2.5 ^{o}C). Then the cables for strain gages and LVDT were wired to a Campbell data logger (CR9000) which sits outside the cold room. The time interval was 10 seconds for displacement measurement. The temperature was obtained by reading the thermistors with a multi-meter. Figure A.18 shows the anchor under loading. The weight was added in one or two minutes for each load stage.

Figure A.18 Backfill the silt slurry into the annular space.

Appendix B: Anchor Load Test Results

Section B.1 lists the loading conditions of all the anchor load tests, focusing on the load stages, duration, temperatures, and anchor status. Section B.1 presents all the creep curves from the anchor load tests.

B.1 Load Conditions

Table 3.1 summarizes the loading conditions for the nineteen anchor load tests (staged-load) conducted in seven periods of time. The "test No." in the table indicates the information about the test period and the type of silt used (e.g., 1-120 means the first test period for silt with a moisture content of 120%). For every stage in each test, Table 3.1 gives the testing date, anchor embedment, applied load and average shear stress, test duration, and variations of temperatures along the anchor (at different depths). Generally, the temperature along the anchor was not equal and there was 0.36 to 1.7 ^{o}F difference between the top and the bottom of the anchor. The temperatures were generally stable during all the load stages, except for the three tests in the second test period. The last column in Table 3.1 also indicated whether the anchors were pulled out or not in each test.

Table B.1 Loading conditions for nineteen anchor load tests.

Test No.	Testing Date	*L*, inch	*P*, kips	*τ*, psi	*t*, hr	*T* °C	Pullout?
1-120	2010/3/3 20:04	23.8	0.9	3	51	-1.1~-1.3	No
--	2010/3/5 23:04	--	1.5	5	72	-0.9~-1.0	No
--	2010/3/8 23:04	--	3.0	10	10	-0.7~-0.9	Yes
2-120	2010/3/25 15:56	23.8	3.3	11.2	77	-0.8~-1.5	No
--	2010/3/28 21:15	--	0.9	3	8.4	-0.1~-0.8	Yes
2-80	2010/3/25 15:56	21.0	0.8	3	72	-0.5~-1.2	No
--	2010/3/28 21:15	--	1.3	5	10	-0.4~-0.5	No
--	2010/4/1 5:34	--	1.8	7	29	-0.3~-0.4	Yes
2-50	2010/3/25 15:56	23.8	0.9	3	77	-0.7~-1.6	No
--	2010/3/28 21:15	--	1.5	5	20	-0.2~-0.5	Yes
3-120	2010/5/1 5:43	23.8	1.6	5.3	5	-1.1~-1.8	No
--	2010/5/1 10:43	--	2.2	7.3	9	-1.2~-1.9	No
--	2010/5/1 19:19	--	2.8	9.3	38	-1.2~-1.8	No
--	2010/5/3 8:55	--	3.4	11.3	7	-1.3~--2.0	No
--	2010/5/3 16:15	--	4.0	13.3	37	-1.3~-2.0	Yes
3-80	2010/4/29 19:53	21.0	2.0	7.4	33.8	-0.8~-1.0	No
--	2010/5/1 5:41	--	2.6	9.6	13.7	-1.1~-1.2	No
--	2010/5/1 19:22	--	3.1	11.8	66.6	-1.2~-1.3	Yes
3-50	2010/5/1 5:54	23.8	1.5	5.1	5	-1.2~-1.9	No
--	2010/5/1 10:48	--	2.1	7.0	9	-1.3~-1.9	No
--	2010/5/1 19:53	--	2.7	8.9	17	-1.4~-1.9	No
--	2010/5/2 12:31	--	3.2	10.8	21	-1.4~-1.9	No
--	2010/5/3 9:16	--	3.8	12.7	19	-1.5~-1.9	No
--	2010/5/4 4:19	--	4.4	14.7	17	-1.6~-1.9	No
--	2010/5/4 21:10	--	5.0	16.6	12	-1.6~-1.9	No
--	2010/5/5 9:20	--	5.5	18.5	12	-1.6~-1.9	No
--	2010/5/5 21:20	--	6.1	20.4	6	-1.6~-1.9	No
--	2010/5/6 3:20		6.7	22.4	6	-1.6~-1.9	No

L, anchor embedment; P, applied load; τ, average shear stress; t, test duration; T variation of temperatures along the anchor.

Table B.1 Loading conditions for nineteen anchor load tests. (cont.)

Test No.	Testing Date	L, inch	P, kips	τ, psi	t, hr	T, °C	Pullout?
4-120	2010/5/17 9:29	23.8	1.5	5.0	9	-1.1~-1.7	No
--	2010/5/17 18:16	--	2.1	7.0	8	-1.1~-1.7	No
--	2010/5/18 2:13	--	2.7	9.2	16	-1.1~-1.8	No
--	2010/5/18 17:45	--	3.3	11.2	29	-1.1~-1.8	Yes
4-80	2010/5/17 9:35	21.0	1.5	5.5	7	-1.0~-1.4	No
--	2010/5/17 16:15	--	2.1	8.0	10	-1.2~-1.4	No
--	2010/5/18 2:11	--	2.7	10.3	14	-1.0~-1.3	Yes
4-50	2010/5/17 9:32	23.8	1.5	5.0	9	-1.0~-1.7	No
--	2010/5/17 18:16	--	2.1	8.0	8	-1.0~-1.7	No
--	2010/5/18 9:56	--	3.8	12.6	23	-1.0~-1.7	No
--	2010/5/19 9:06	--	4.9	16.4	13	-1.0~-1.7	Yes
5-120	2010/5/28 7:56	23.8	0.9	3	6	-0.1~-0.2	Yes
5-80	2010/5/28 7:56	21	0.8	3	23	-0.6~-0.8	No
--	2010/5/29 6:56	--	1.3	4.8	23	-0.6~-0.9	Yes
5-50	2010/5/28 7:56	23.8	0.9	3.0	23	-1.0~-1.6	No
--	2010/5/29 6:56	--	1.7	5.8	32	-1.0~-1.7	No
--	2010/5/30 14:56	--	2.4	8.0	23	-1.0~-1.6	No
--	2010/5/31 13:56	--	3.1	10.5	10	-1.1~-1.6	No
--	2010/5/31 23:56	--	3.9	13.2	24	-1.2~-1.7	Yes
--	2010/6/1 23:56	--	4.7	15.8	2	-1.3~1.6	Yes
6-120	2010/6/15 10:05	23.8	2.8	9.4	42	-2.7~-3.3	No
--	2010/6/17 3:46	--	4.2	14.1	24	-2.7~-3.1	No
--	2010/6/18 3:58	--	5.8	19.4	66	-2.7~-3.1	Yes
6-80	2010/6/15 10:05	21.0	2.8	10.7	42	-2.4~-2.6	No
--	2010/6/17 3:46	--	4.1	15.6	53	-2.2~-2.5	No
--	2010/6/19 8:28	--	5.3	19.9	67	-2.2~-2.4	Yes
6-50	2010/6/15 10:05	23.8	2.7	8.9	132	-2.1~-2.5	No
--	2010/6/20 22:16	--	5.5	18.4	29	-2.3~-2.9	Yes
7-120	2010/6/25 7:40	23.8	2.0	6.8	24	-0.7~-1.3	No
--	2010/6/26 7:40	--	3.0	10.1	4	-0.8~-1.1	Yes
7-80	2010/6/25 7:40	21.0	1.6	6.2	24	-0.7~-0.8	No
--	2010/6/26 7:40	--	2.4	9.2	4	-0.6~-0.7	Yes
7-50	2010/6/25 7:40	23.8	1.9	6.3	24	-0.4~-1.0	No
--	2010/6/26 7:40	--	2.8	9.5	13	-0.4~-0.9	Yes

B.2 Creep Curves from the Nineteen Load Tests

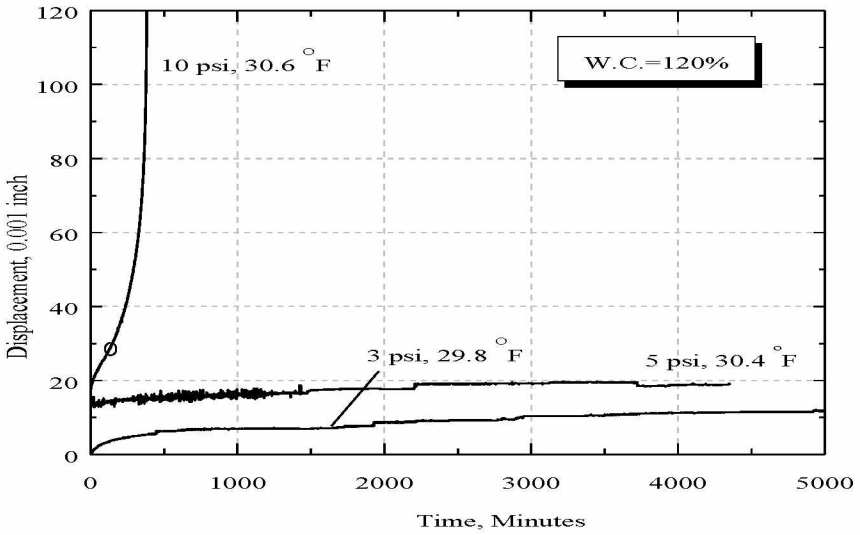

(a)

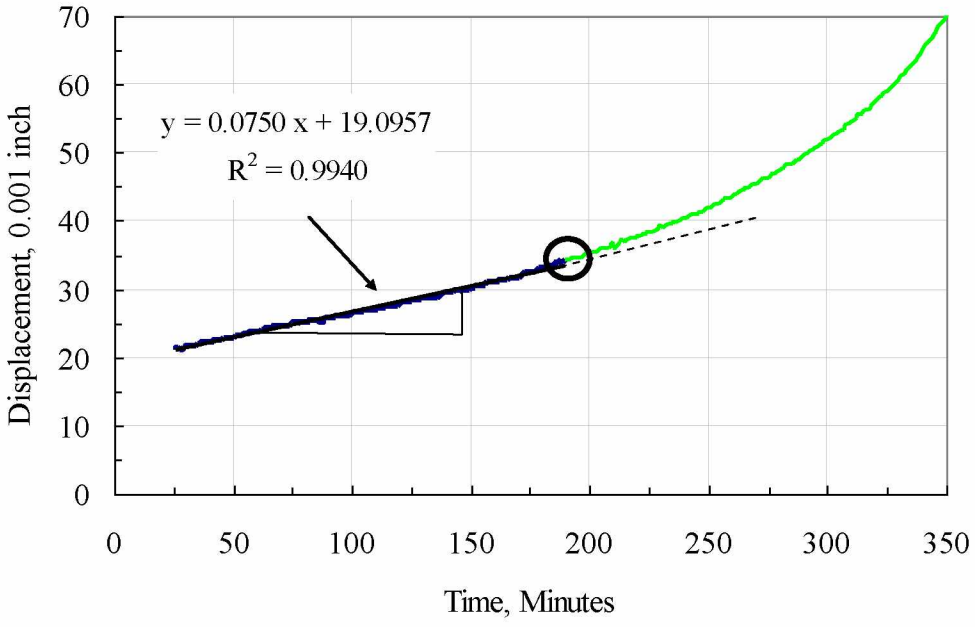

(b)

Figure B.1 Test results for test #1-120. (a) Creep curves at all stages. (b) minimum displacement rate and onset of tertiary creep at shear stress = 10 psi.

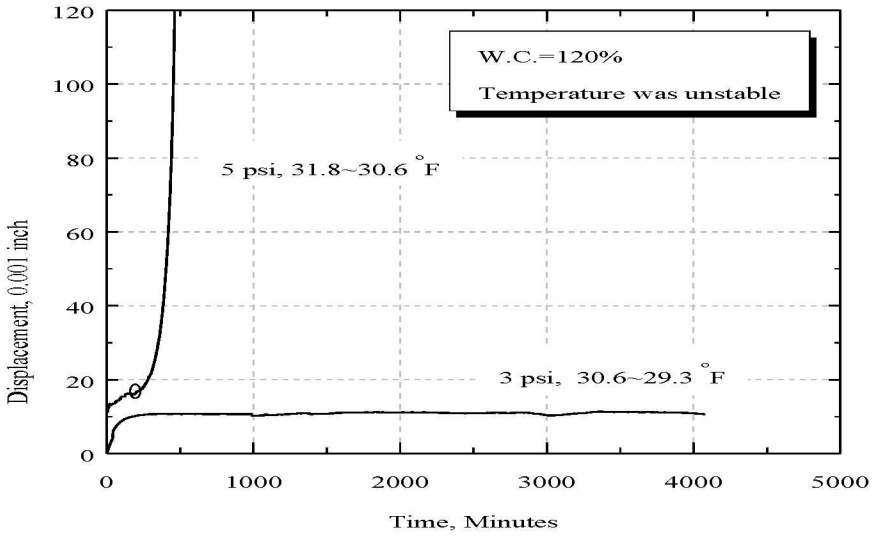

(a)

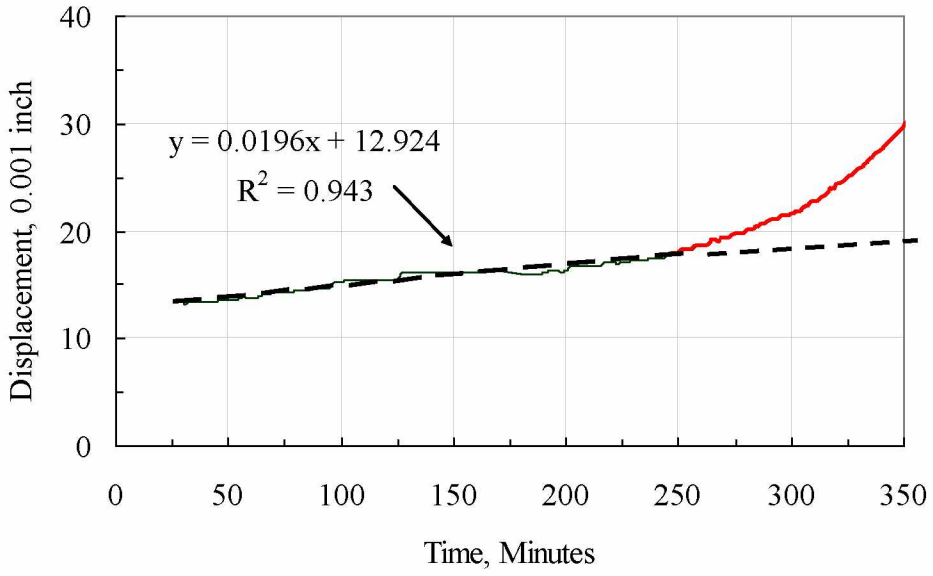

(b)

Figure B.2 Test results for test #2-120. (a) Creep curves at all stages. (b) minimum displacement rate and onset of tertiary creep at shear stress = 5 psi.

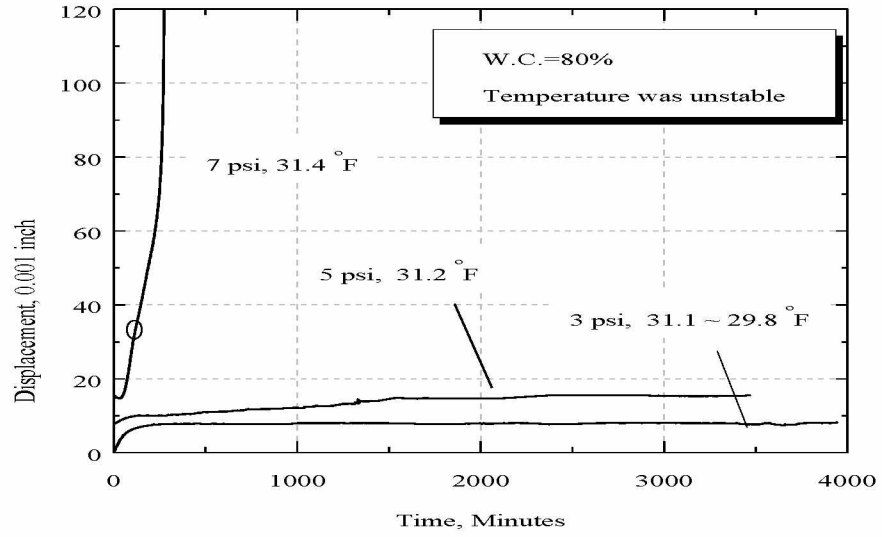

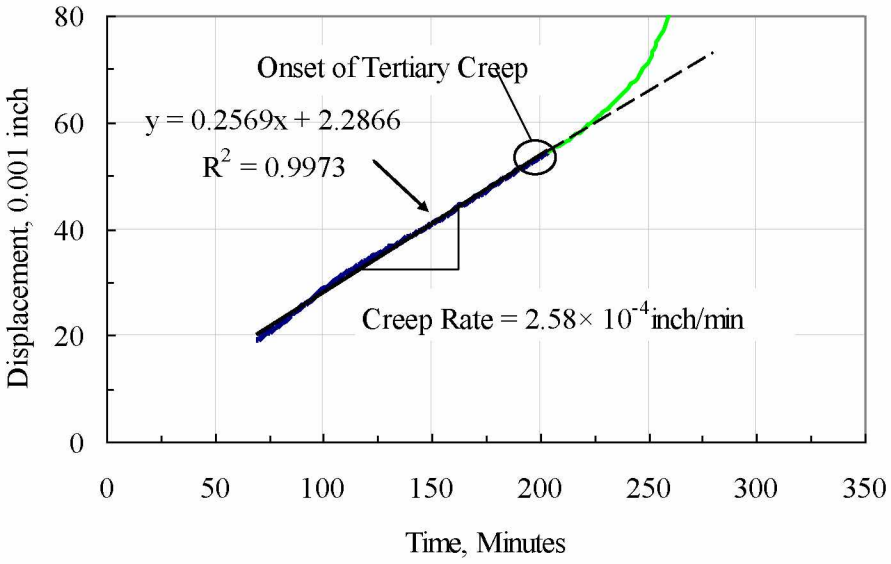

(b)

Figure B.3 Test results for test #2-80. (a) Creep curves at all stages. (b) minimum displacement rate and onset of tertiary creep at shear stress = 7 psi.

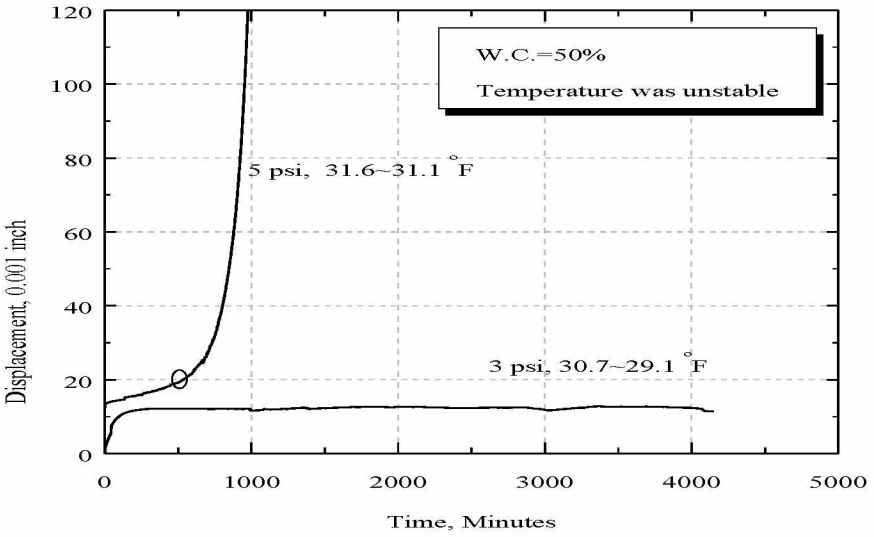

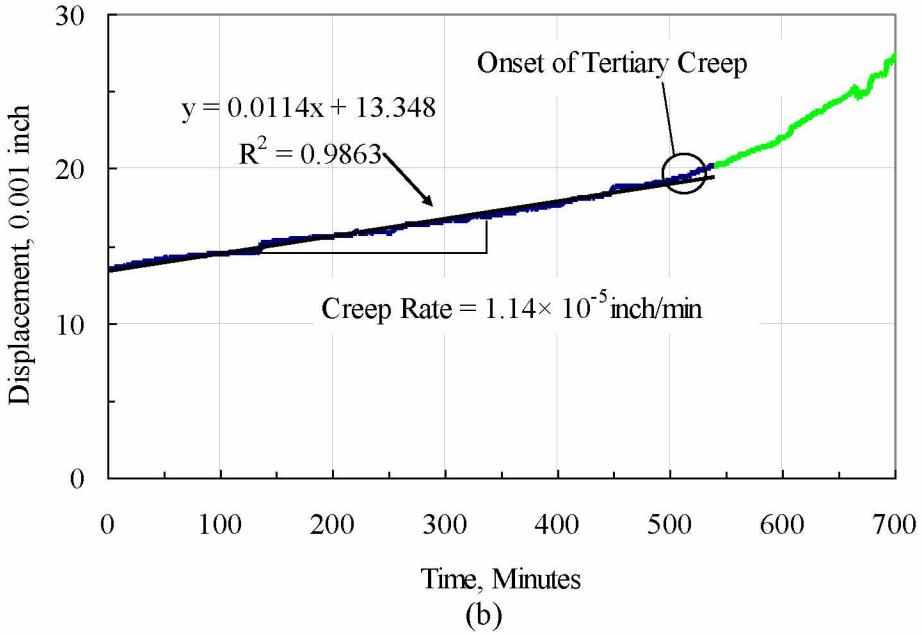

(b)

Figure B.4 Test results for test #2-50. (a) Creep curves at all stages. (b) minimum displacement rate and onset of tertiary creep at shear stress = 5 psi.

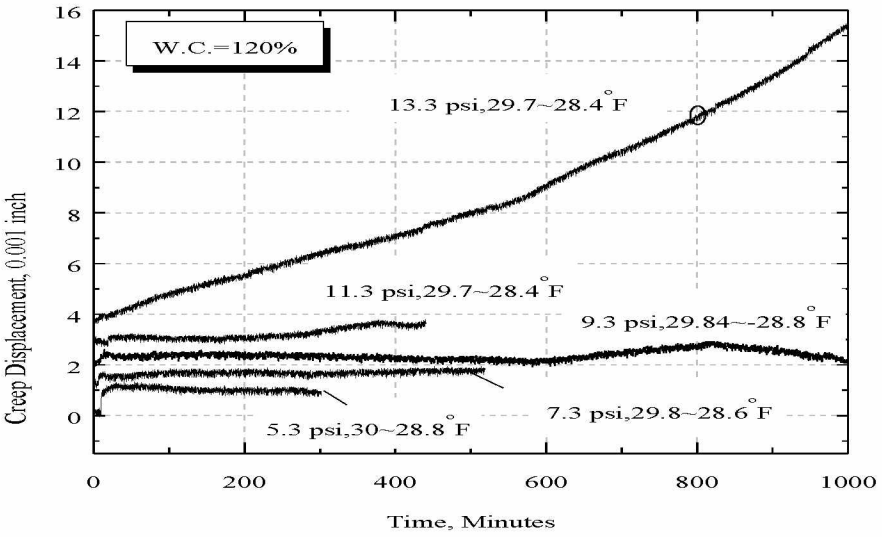

(a)

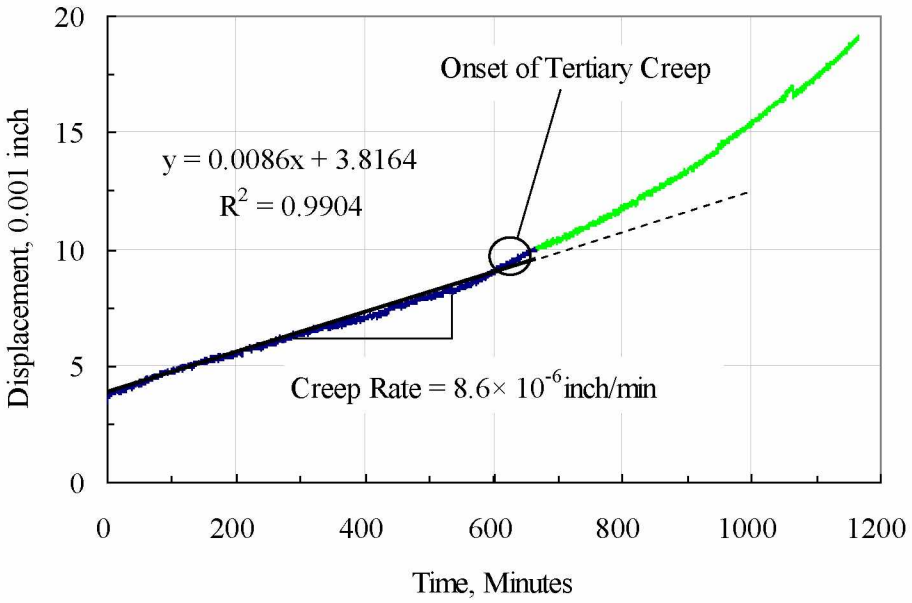

(b)

Figure B.5 Test results for test #3-120. (a) Creep curves at all stages. (b) minimum displacement rate and onset of tertiary creep at shear stress = 13.3 psi.

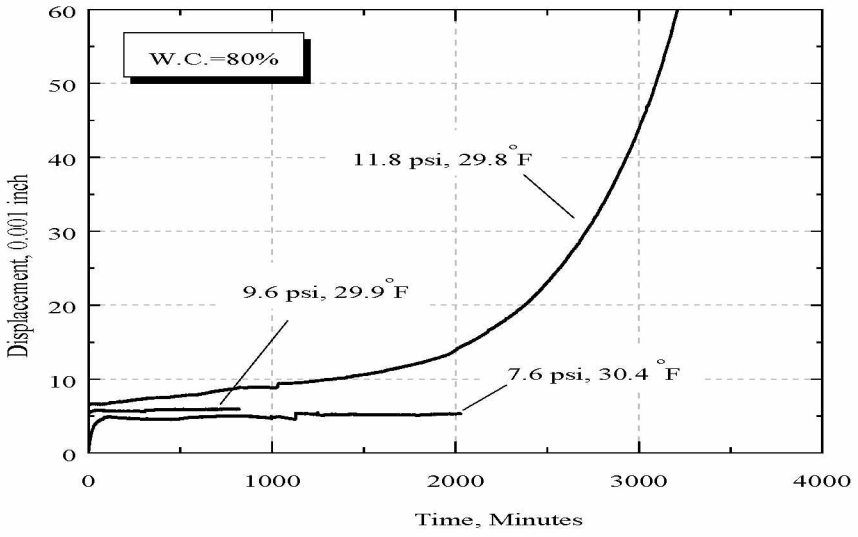

(a)

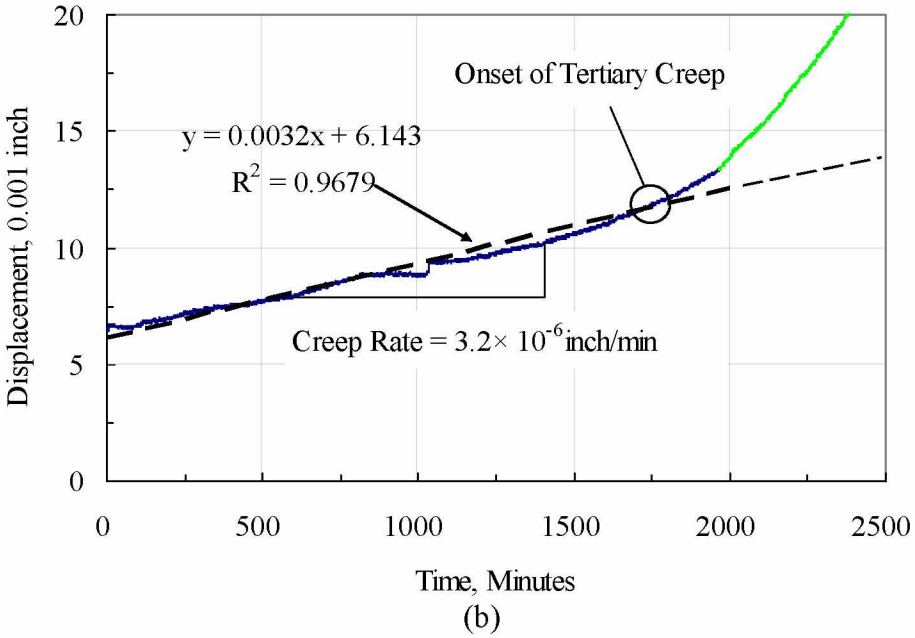

(b)

Figure B.6 Test results for test #3-80. (a) Creep curves at all stages. (b) minimum displacement rate and onset of tertiary creep at shear stress = 11.8 psi.

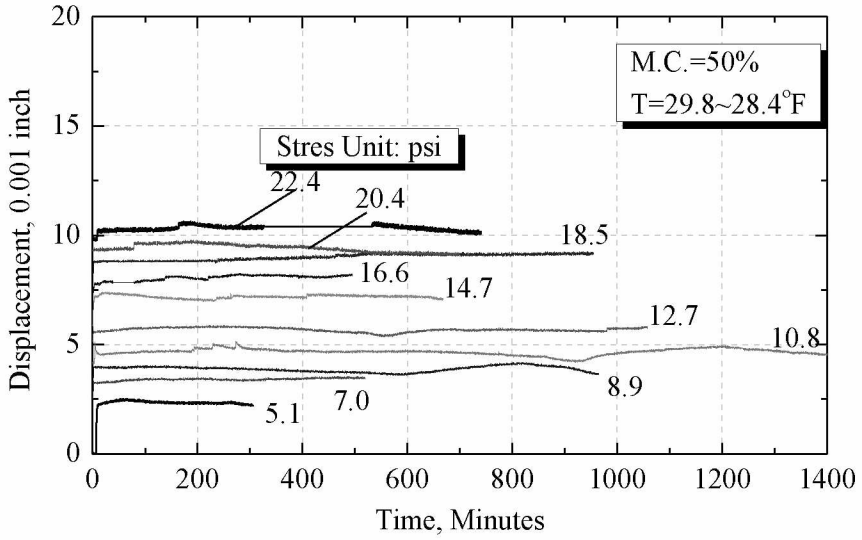

Figure B.7 Test results for test #3-80.

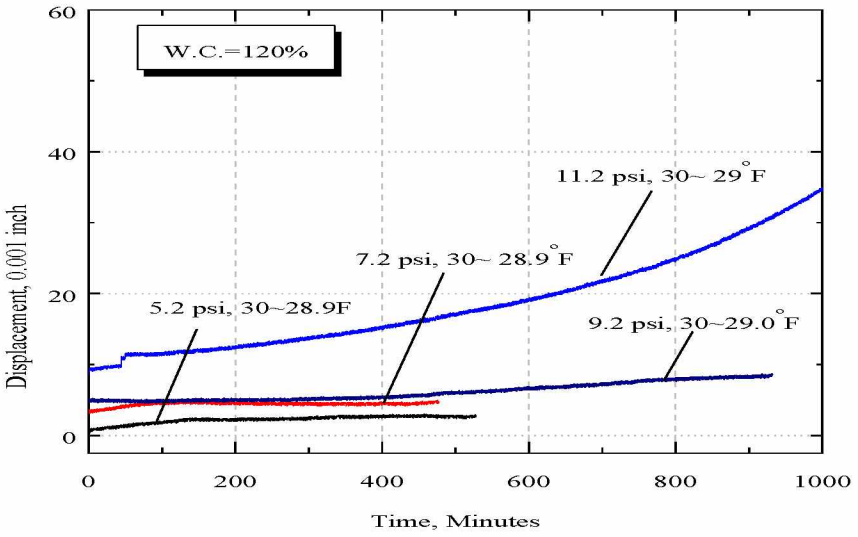

(a)

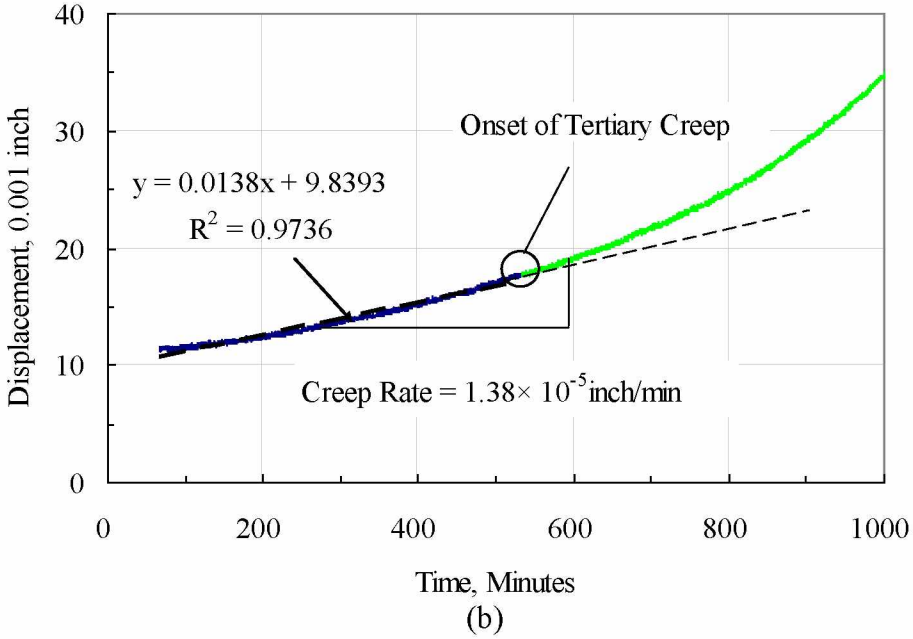

(b)

Figure B.8 Test results for test #4-120. (a) Creep curves at all stages. (b) Minimum displacement rate and onset of tertiary creep at shear stress = 11.2 psi.

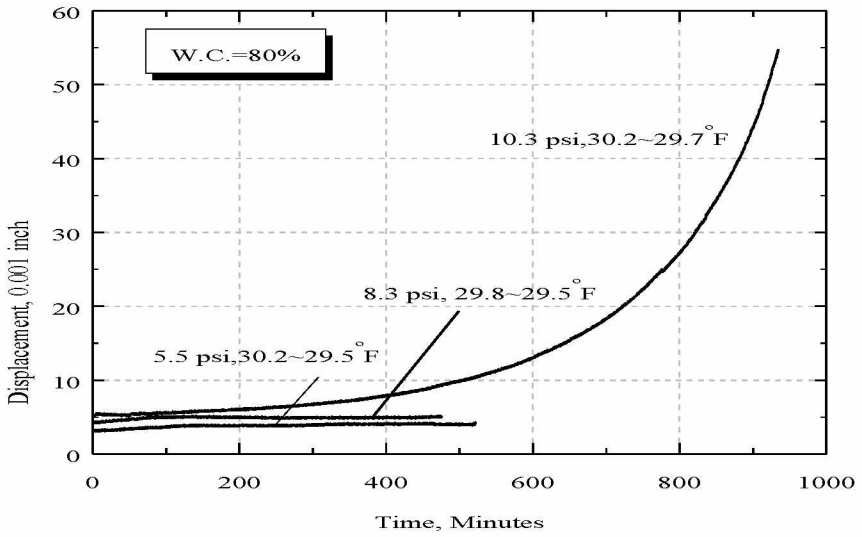

(a)

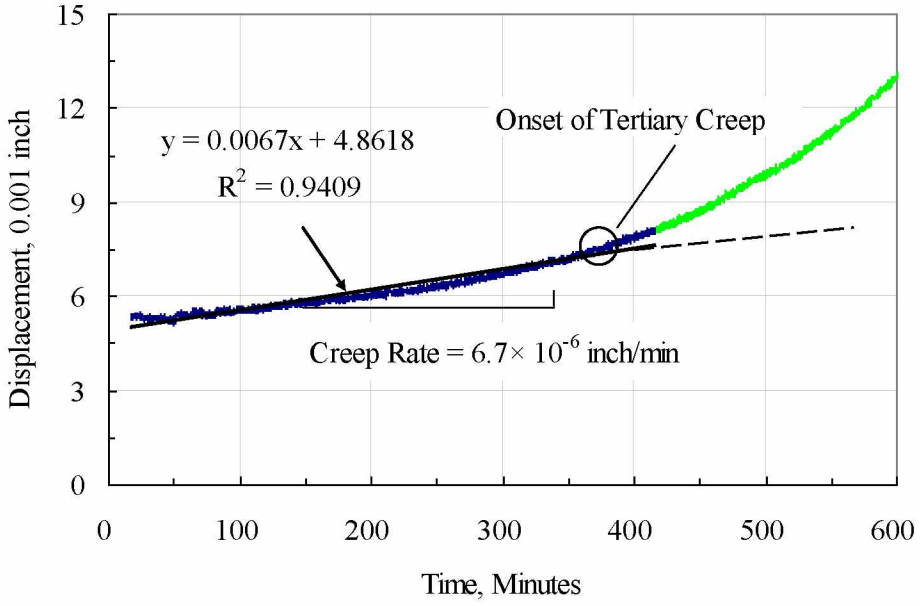

(b)

Figure B.9 Test results for test #4-80. (a) creep curves at all stages. (b) minimum displacement rate and onset of tertiary creep at shear stress = 10.3 psi.

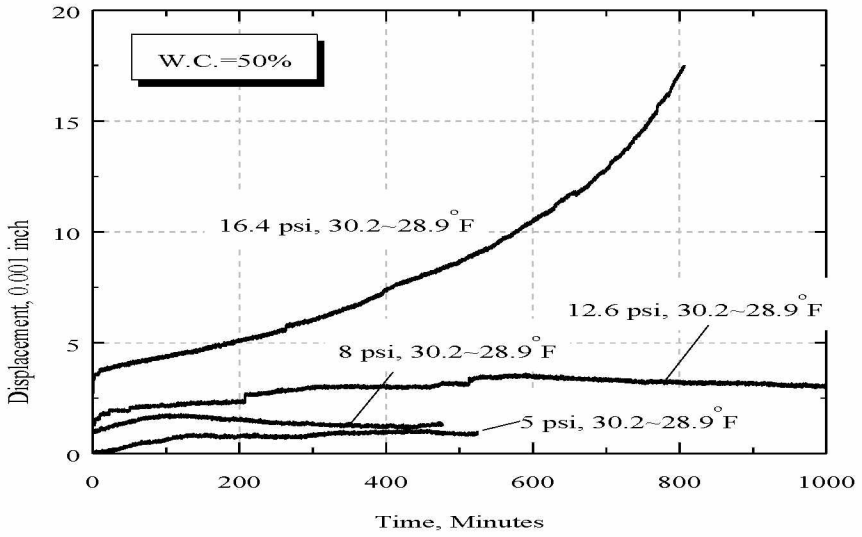

(a)

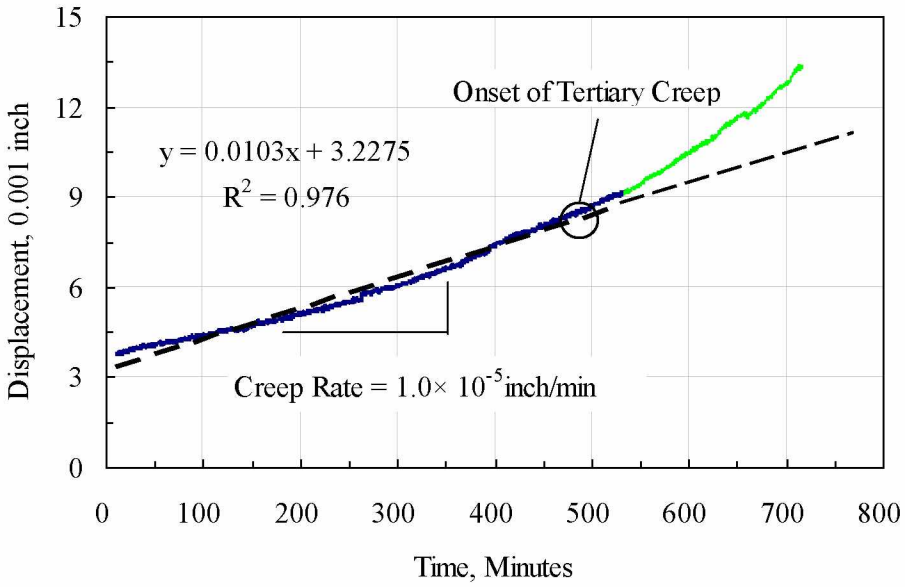

(b)

Figure B.10 Test results for test #4-50. (a) Creep curves at all stages. (b) minimum displacement rate and onset of tertiary creep at shear stress = 16.4 psi.

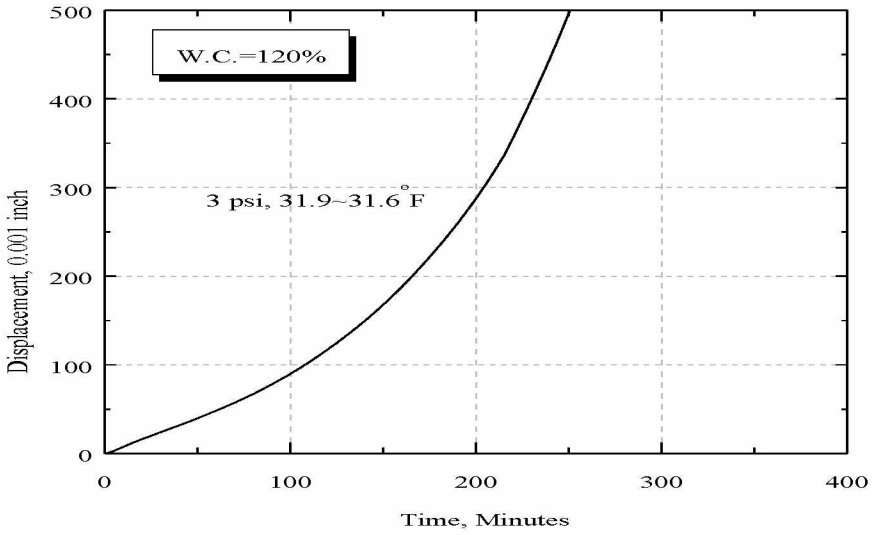

(a)

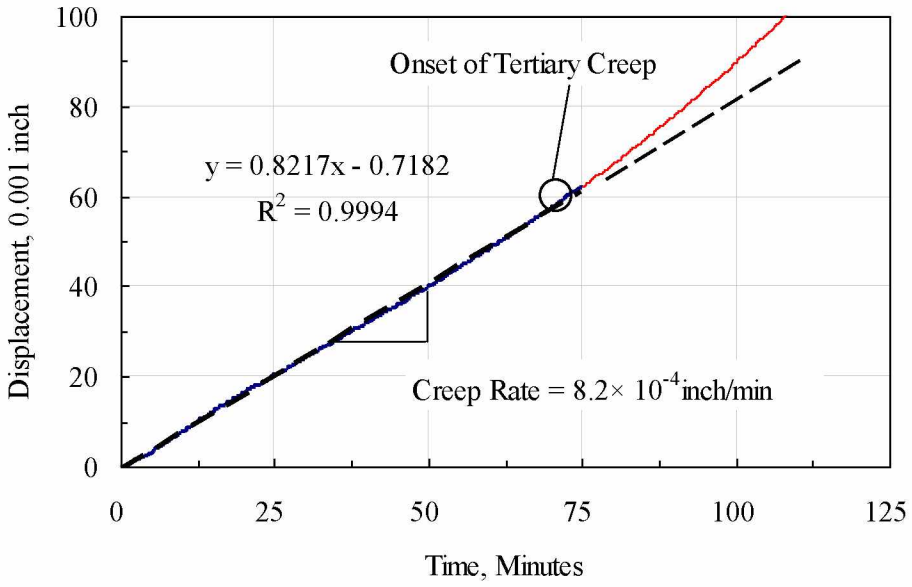

(b)

Figure B.11Test results for test #5-120. (a) Creep curves at all stages. (b) minimum displacement rate and onset of tertiary creep at shear stress = 3 psi.

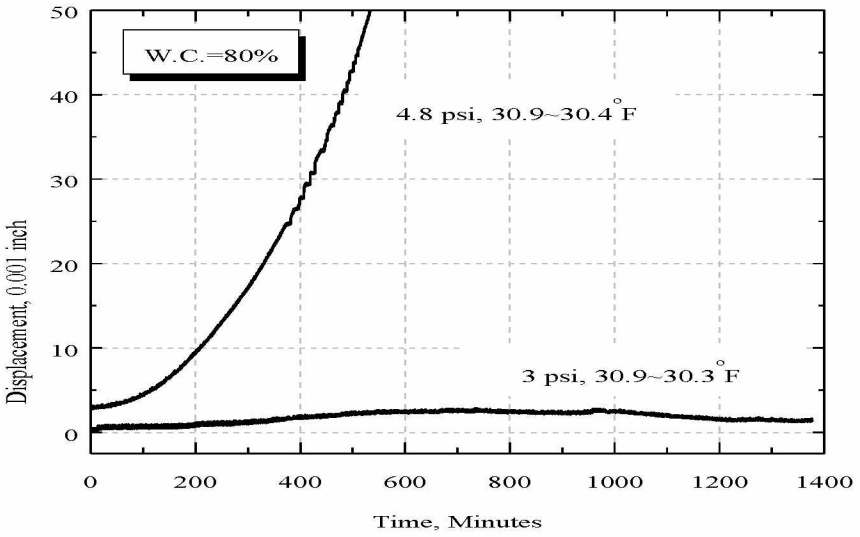

(a)

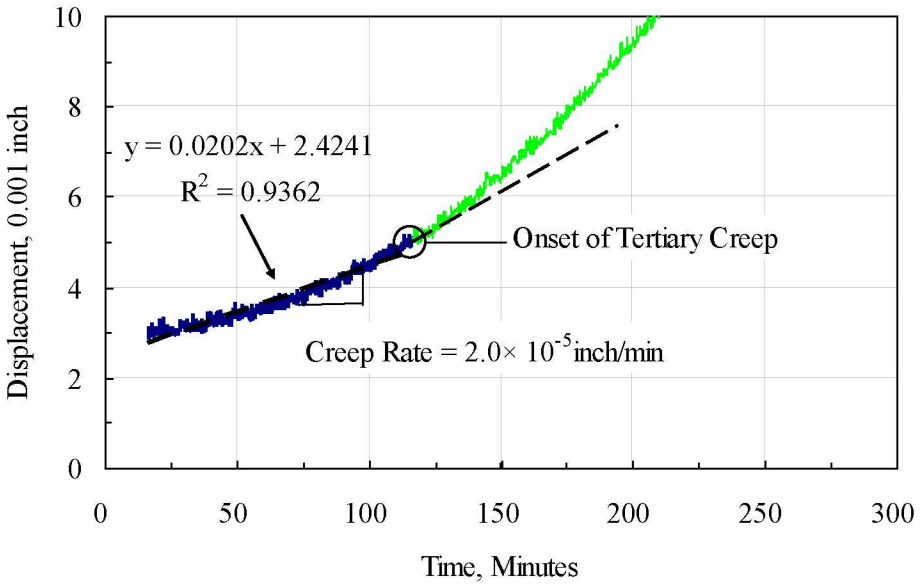

(b)

Figure B.12 Test results for test #5-80. (a) creep curves at all stages. (b) minimum displacement rate and onset of tertiary creep at shear stress = 4.8 psi.

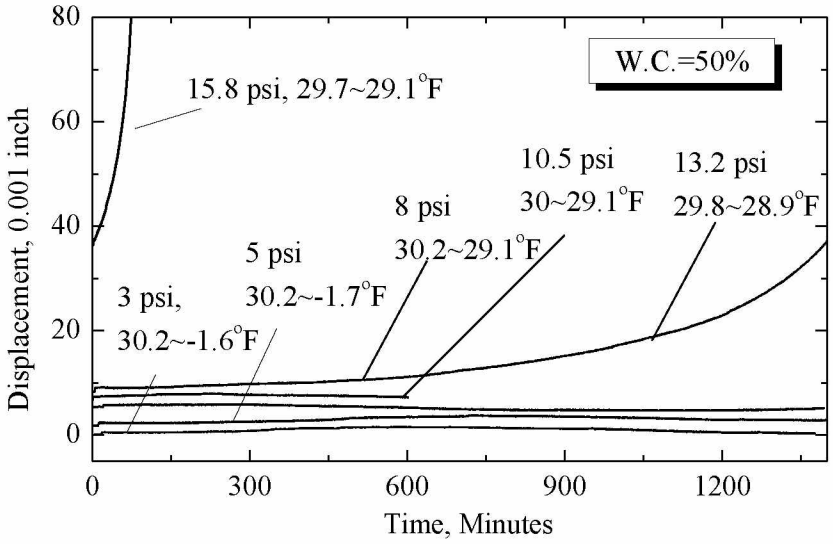

(a)

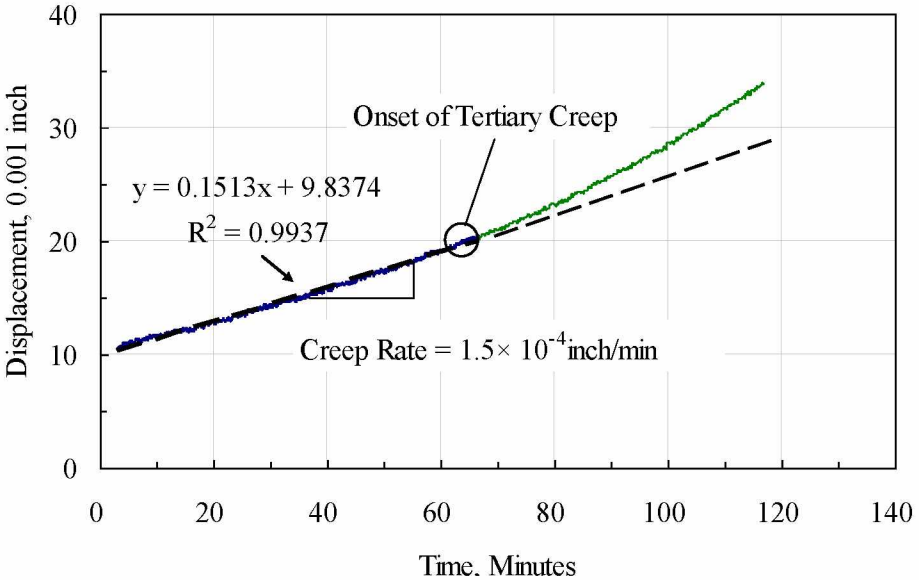

(b)

Figure B.13 Test results for test #5-50. (a) Creep curves at all stages. (b) minimum displacement rate and onset of tertiary creep at shear stress = 13.2 psi.

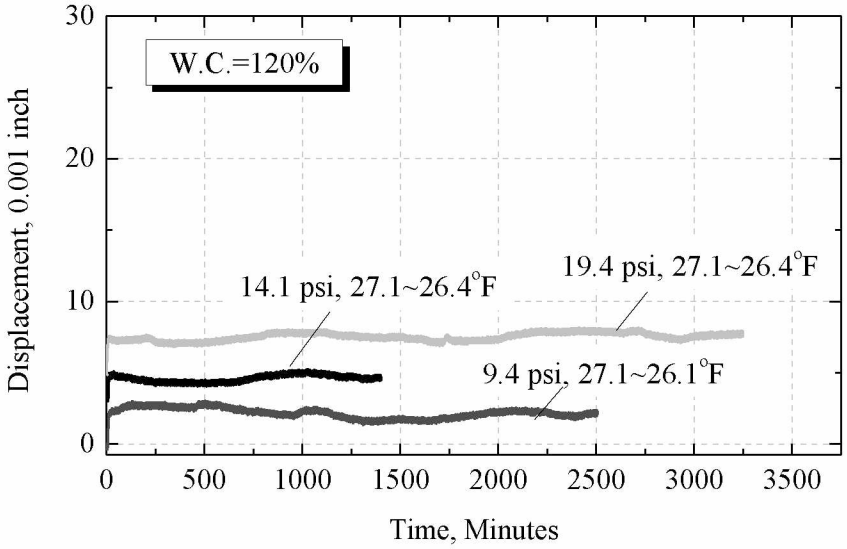

Figure B.14Test results for Test # 6-120.

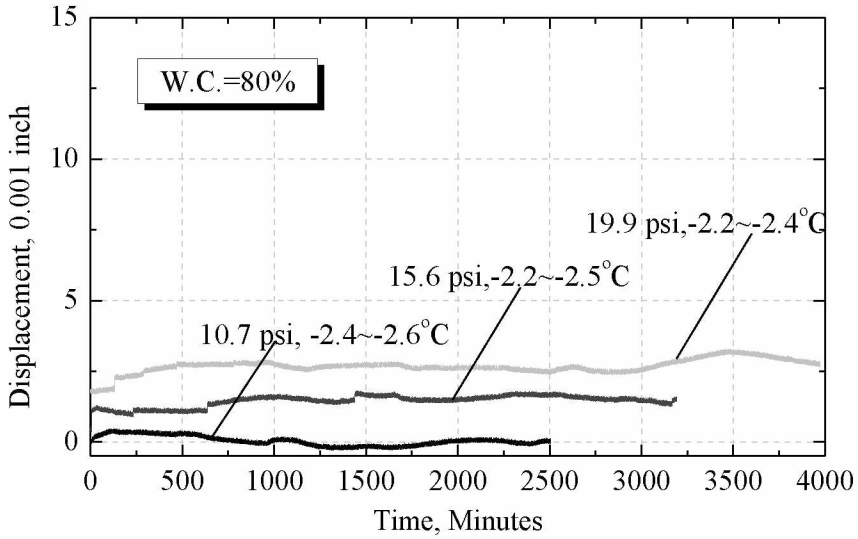

Figure B.15 Test results for Test # 6-80.

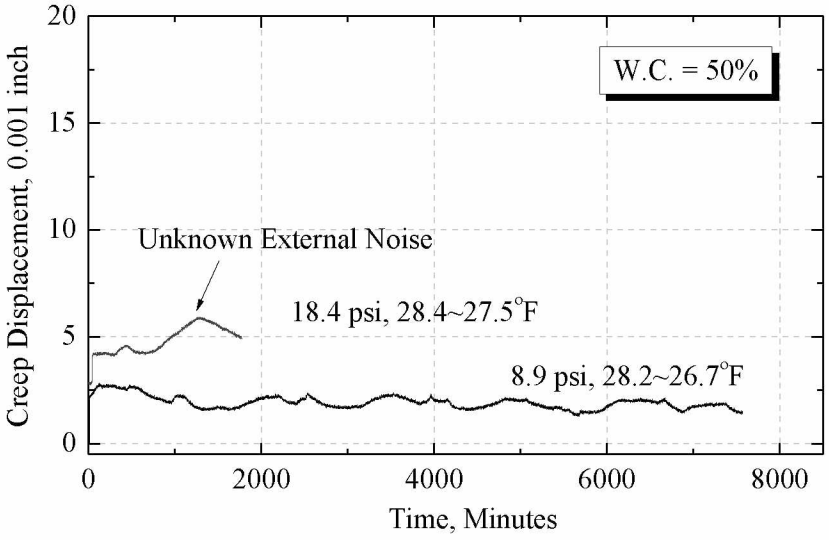

Figure B.16 Test results for Test # 6-50.

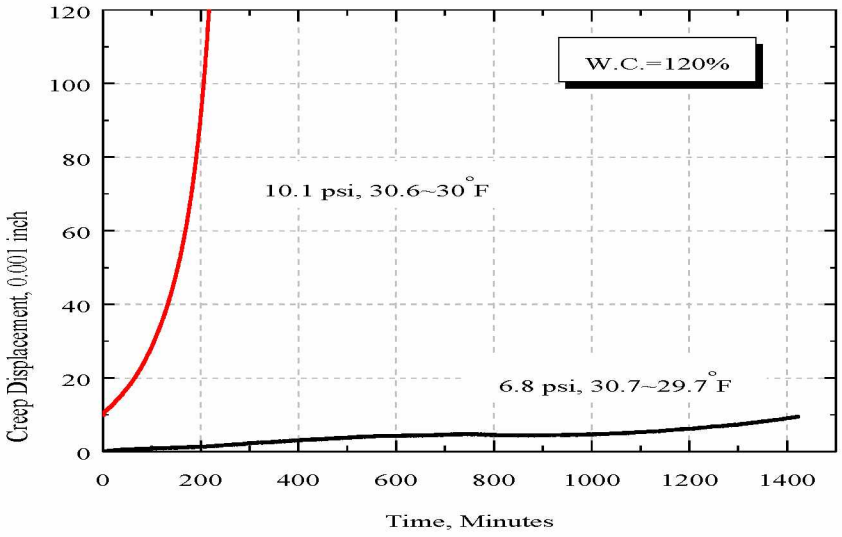

(a)

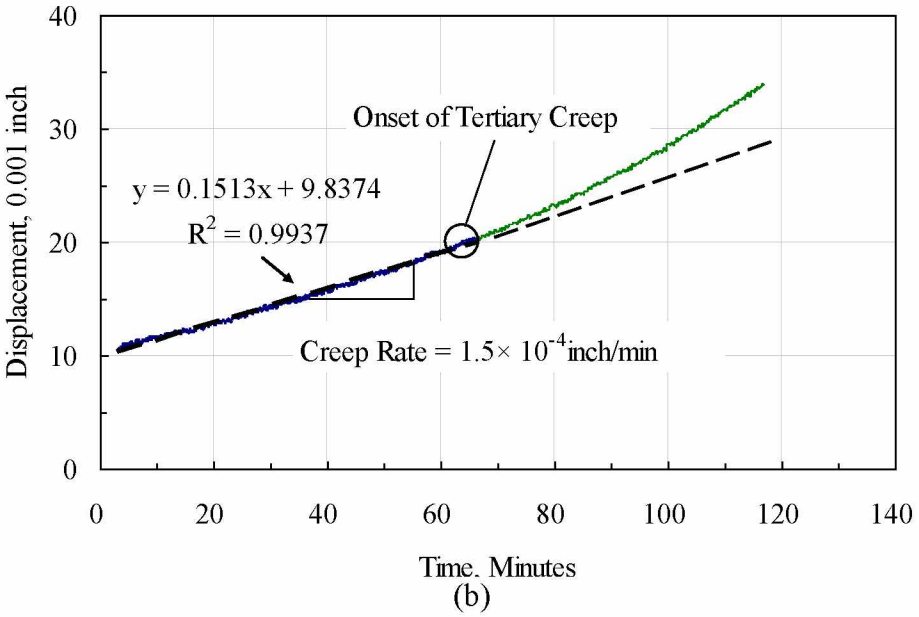

(b)

Figure B.17 Test results for test #7-120. (a) Creep curves at all stages. (b) minimum displacement rate and onset of tertiary creep at shear stress = 10.1 psi.

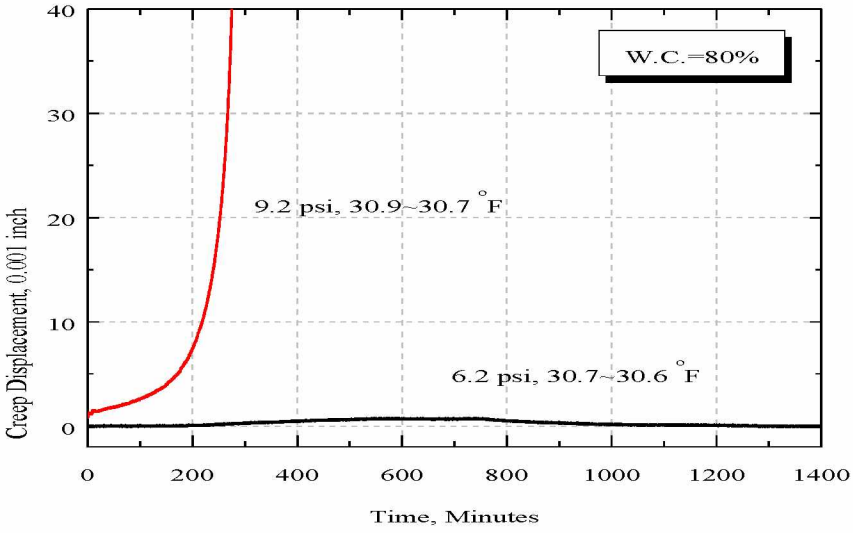

(a)

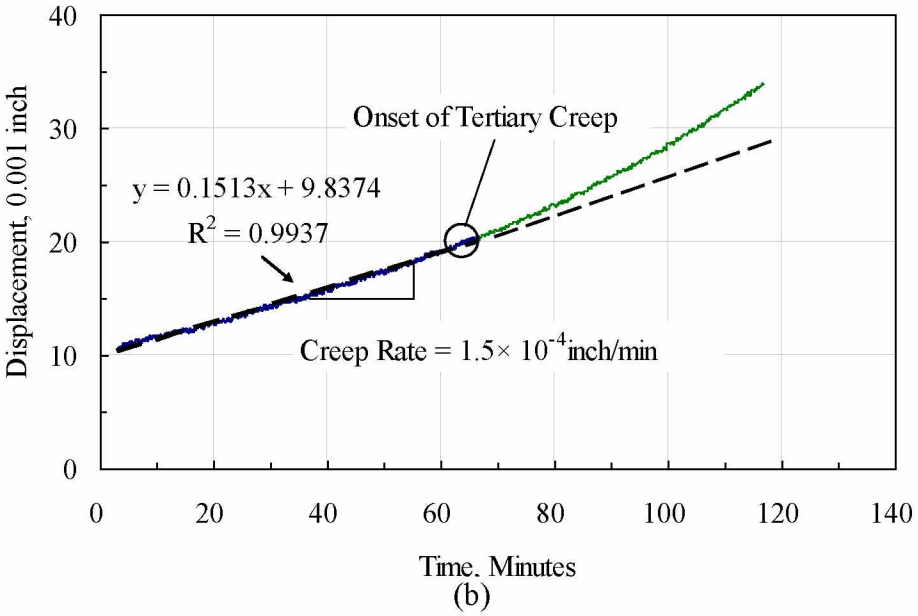

(b)

Figure B.18 Test results for test #7-80. (a) creep curves at all stages. (b) minimum displacement rate and onset of tertiary creep at shear stress = 9.2 psi.

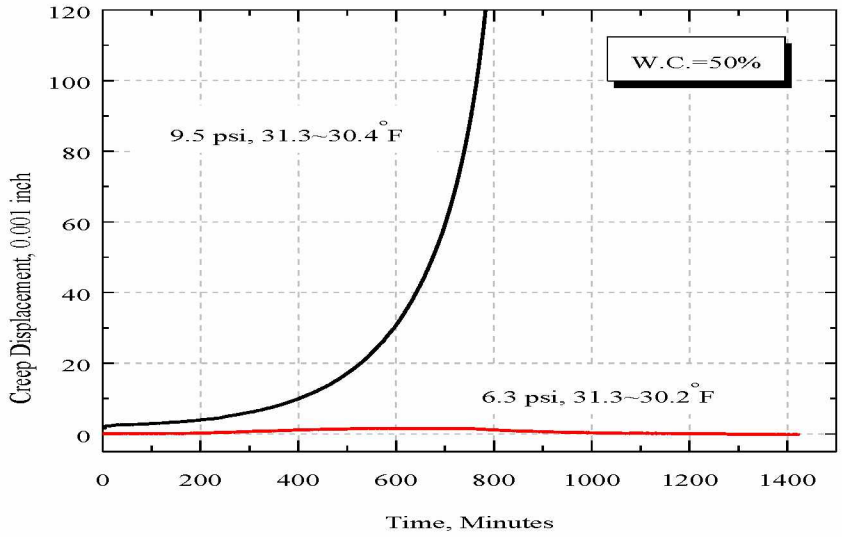

(a)

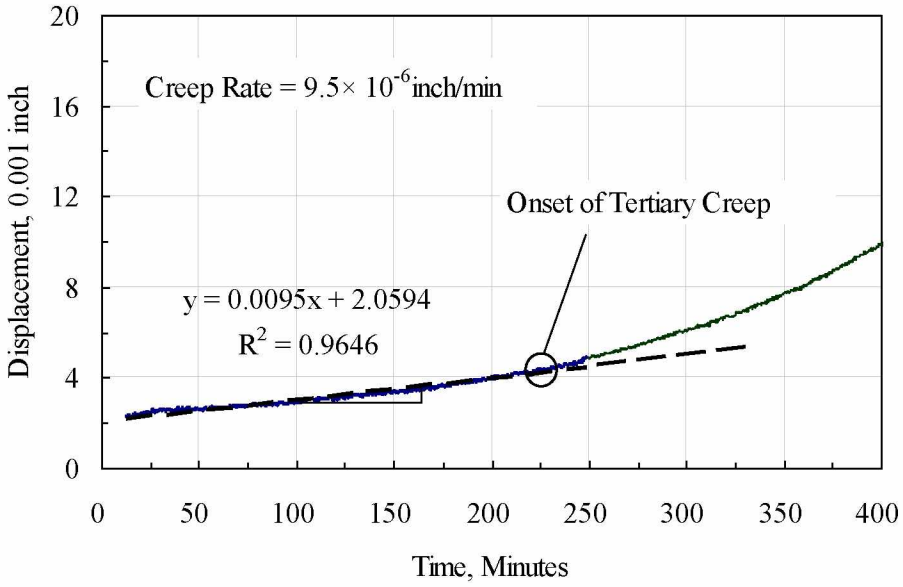

(b)

Figure B.19 Test results for test #7-50. (a) creep curves at all stages. (b) minimum displacement rate and onset of tertiary creep at shear stress = 9.5 psi.

Appendix C: Data Regression Results

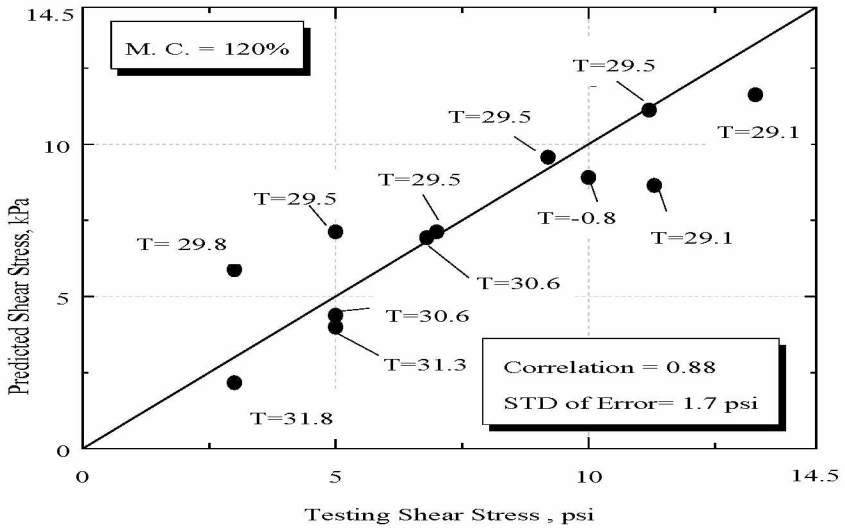

Figure C.1 Regression result for M.C. = 120%. T is temperature in Fahrenheit.

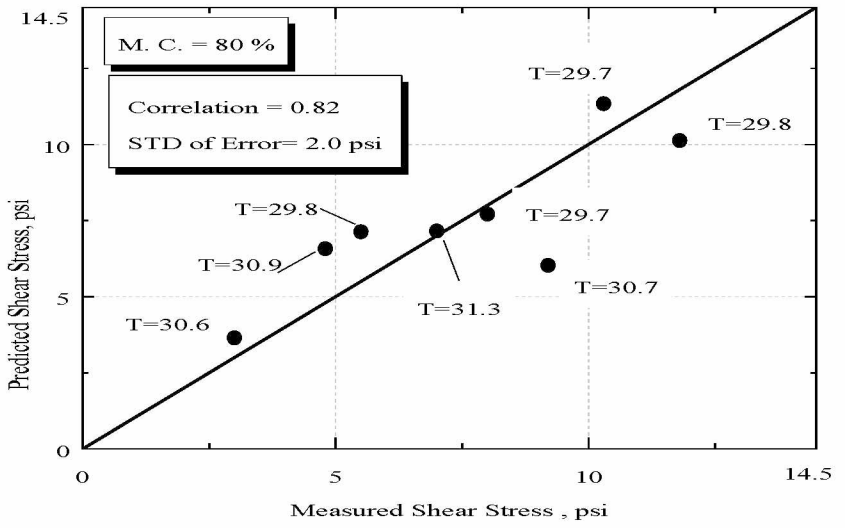

Figure C.2 Regression result for M.C. = 80%. T is temperature in Fahrenheit.

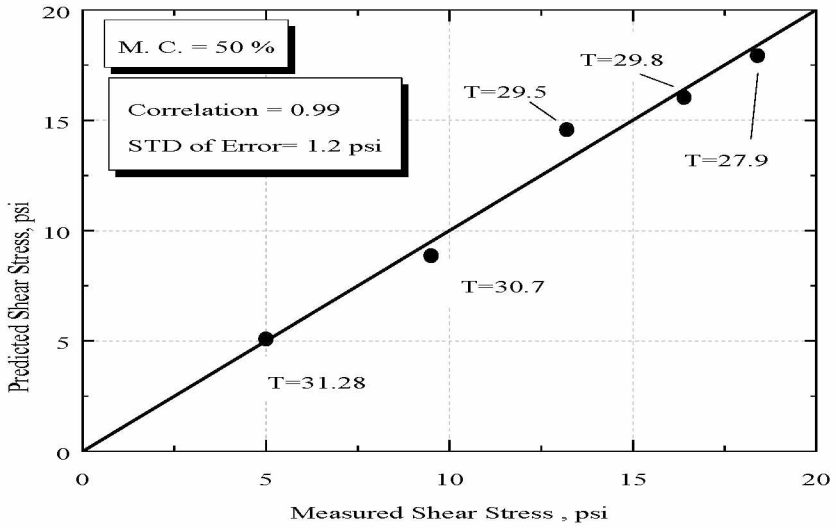

Figure C.3 Regression result for M.C. 50%. T is temperature in Fahrenheit.